Energy & Buildings 187 (2019) 144–162

Contents lists available at ScienceDirect

Energy & Buildings

journal homepage: www.elsevier.com/locate/enbuild

Effectiveness of cool walls on cooling load and urban temperature in a tropical climate

Negin Nazarian[a,b,*], Nathalie Dumas[b], Jan Kleissl[c], Leslie Norford[d]

[a] University of New South Wales, Sydney, Australia
[b] Singapore-MIT Alliance for Research and Technology, Singapore
[c] Department of Mechanical and Aerospace Engineering, University of California, San Diego, USA
[d] Department of Architecture, Massachusetts Institute of Technology, USA

ARTICLE INFO

Article history:
Received 14 June 2018
Revised 8 November 2018
Accepted 17 January 2019
Available online 22 January 2019

Keywords:
Cool walls
Reflective surfaces
Building energy use
Urban heat island
Urban design

ABSTRACT

The urban overheating, driven by the increasing expansion of our cities and the global climate change, is becoming one of the main environmental challenges of today. Consequently, cooling technologies are emerging as mitigation and adaptation strategies. Reflective roof and pavement surfaces have been widely studied for their potential benefits, but detailed evaluations of the effect of wall albedo on the urban microclimate are limited. This study addresses this gap by evaluating the effects of reflective walls on urban energy use and outdoor climate. The energy balance of an idealized neighborhood is represented using a 3D numerical model, Temperature of Urban Facets Indoor-Outdoor Building Energy Simulator (TUF-IOBES), which determines the cooling loads and outdoor air temperature. The study focuses on the tropical climate of Singapore, addressing the urban climate in highly-populated cities in low latitudes that are significantly affected by the UHI. Simulations are conducted for two neighborhoods representative of low-rise residential and high-rise commercial urban areas, spanning a range of urban density, canyon geometry, building construction, and occupant schedules. The building thermal load and outdoor temperature are then calculated for these two idealized neighborhoods, analyzing the effectiveness of cool walls while also considering the role of other design factors such as window-to-wall ratio (WWR) and glazing solar heat gain coefficient (SHGC) in modulating the impact. Unlike the analysis of cool roofs, we find that a universal conclusion regarding the impact of cool walls cannot be drawn. The role of wall albedo significantly depends on the collective design of urban areas as well as the use and occupancy of buildings. We find that urban density (in other words the local climate zone) followed by window properties are important factors in determining the impact of wall albedo on thermal loads and UHI, as they determine the radiative exchange between and into the buildings. Accordingly, contrary to the general expectation, for a high urban density (commercial neighborhood LCZ6) and high WWR and SHGC, we observe that cool (reflective) walls can increase the building energy use. Regarding UHI, increasing the reflectivity of walls decreases the canopy air temperature but the impact is marginal ($\sim$0.1 °C) compared to other urban design parameters.

1. Introduction

With an expected 20% increase of the urban population by 2050, our world is subjected to the fastest rate of urbanization in history [12]. The urban overheating, often described by Urban Heat Island (UHI) phenomenon, is a major environmental challenge directly resulting from this urban expansion, which corresponds to a significantly higher urban air temperature (1 °C to 3 °C, on average, reported by Grimmond [18]) compared to the "rural" or less-urbanized surroundings. Thermal and radiative properties of urban materials, waste heat due to human activities (anthropogenic heat), as well as reduced wind speed and trapping of long-wave radiation are the principal factors contributing to the urban heating [38], while plant cover and soil moisture evaporation, representative of the rural areas, can no longer moderate this temperature modification. Under specific meteorological conditions, UHI can reach more than 10 °C [18,56] and a maximum of 12.9 °C has been observed in Phoenix, Arizona, during April 2002 [56]. The ensuing effects of urban overheating are then twofold: (1) with the increase in outdoor temperature during cooling seasons, building

* Corresponding author. UNSW Built Environment, UNSW Sydney, Room 2023, Level 2, Red Centre West Wing (H13), NSW 2052, Australia
E-mail address: n.nazarian@unsw.edu.au (N. Nazarian).

https://doi.org/10.1016/j.enbuild.2019.01.022
0378-7788/

Nomenclature

Abbreviations

AC	air-conditioning system
AR	canyon aspect ratio
BCA	building construction authority, Singapore
COM	commercial neighborhood
HVAC	heating, ventilation, and air conditioning
LCZ	local climate zone (Stewart and Oke, 2012)
RES	residential neighborhood
SHGC	solar heat gain coefficient
TUF-IOBES	temperature of urban facades indoor-outdoor building energy simulator (Yaghoobian and Kleissl, 2012b)
UBL	urban boundary layer
UHI	urban heat island
UWG	urban weather generator (Bueno et al., 2013)
WWR	window-to-wall ratio

Greek symbols

α	surface albedo
λ_p	plan area density

Roman symbols

A	building floor area (m)
L	building length (m)
W	canopy width (m)
H	building height (m)
Q_A	sensible waste heat rejected into the canyon ($W.m^{-2}$)
Q_{CE}	convective portion of internal loads ($W.m^{-2}$)
Q_{conv}	conduction heat transfer through the walls ($W.m^{-2}$)
Q_{conv}	convection heat transfer from the surfaces to air ($W.m^{-2}$)
Q_H	convection heat transfer from building and ground surfaces ($W.m^{-2}$)
Q_{IV}	sensible load due to infiltration ($W.m^{-2}$)
Q_{LWS}	net longwave radiation flux from equipment, people, and lights in a zone ($W.m^{-2}$)
Q_{LWX}	net longwave radiant exchange flux between zone surfaces ($W.m^{-2}$)
Q_{sol}	transmitted solar radiation flux absorbed on indoor surfaces ($W.m^{-2}$)
Q_{SW}	net shortwave radiation flux to the surface from interior light ($W.m^{-2}$)
Q_{sys}	heat transfer to/from the HVAC system ($W.m^{-2}$)
Q_T	sensible heat flux exchanged with the above canopy layer ($W.m^{-2}$)
T_{can}	canopy air temperature (°C)
T_{ubl}	air temperature at UBL (°C)

energy demand increases significantly [41], and (2) peoples sensation of the thermal environment, i.e. thermal comfort, is affected. The latter raises concerns about thermal-related vulnerability and human health in cities, as high ambient air temperatures are associated with an increase in mortality rates [22,44]. Therefore, it is paramount that the investigation of mitigation strategies for urban heating should consider both aspects of indoor and outdoor environments in cities, such as canopy air temperature and building energy use, as well as the possible interaction between the two.

The urban heating mitigation strategies proposed in built environments are differentiated in several categories, including urban vegetation, urban water bodies, enhanced shading, reflective materials, and materials with high optical and thermal performance [56]. Among them, reflective or cool materials as well as vegetated (green) surfaces have been widely studied, and considered as effective methods for decreasing not only building thermal loads, but also ambient air temperature [30,45]. A 0.10 albedo increase of 65.4% of worldwide land area (between 45°N and 45°S) is estimated to decrease global temperature by more than 2 °C in about 20 years [1]. Accordingly, various methodologies have been developed for increasing wall albedo with different levels of complexity. For example, light-color coating or painting techniques can be applied to all types of building surfaces for increasing the albedo. For obtaining cool urban pavements, an albedo increase of about 0.15 can be reached by using chip seal or slurry coating instead of asphalt [42]. In addition to traditional cool materials, new advanced materials and technologies are also emerging, including the development of retro-reflective materials (i.e. engineered materials to preferentially reflect incident light back towards its source regardless of the direction of incidence as proposed by Rossi et al. [36] and Castellani et al. [8]) which have been evaluated (experimentally and numerically) as an effective strategy for mitigating the urban heat [28]; and development of materials capable of self-cleaning or obtaining very high reflectivity values up to 0.94 for artificial white materials, against a maximum of 0.75 with natural products [43].

The benefits of reflective roofs have also been well studied. For the hot-arid climate of Phoenix in Arizona, Salamanca et al. [40] reported that with the maximum coverage rate, i.e. 100% of the roofs covered with highly reflective membranes, the average daily citywide cooling energy demand and near-surface air temperature can be reduced up to 14% and 0.8 °C, respectively. Synnefa et al. [48] demonstrated that increasing the roof solar reflectance can reduce cooling loads by 18–93% and peak cooling demand in air-conditioned buildings by 11–27%. Similarly, due to the broad environmental benefits of green roofs (including the reduction of building energy consumption, mitigation of urban heat island effect, improvement of air pollution, water management, increase of sound insulation, and ecological preservation), their use as an active mitigation measure in urban environments have been promoted [2,30]. From the urban energy and UHI perspective, it is observed that although the environmental benefits of green roofs is intertwined with the types of roofs (indicated by the ground/soil depth and vegetation type) and the climate, it nonetheless can be an effective way in both reducing building energy consumption and mitigating the urban heat island. Olivieri et al. [32] demonstrated that a densely planted green roof reduced building cooling consumption by 60% in a Mediterranean climate, even though the roof was substantially insulated. A recent study summarizing the environmental benefits of green roofs [2] indicates that green roofs are highly efficient in reducing the variation of indoor temperature and decreasing building energy consumption both in warm and cold climates, and concludes that air temperature can be reduced by 0.3 °C–3 °C if large-scale application of green roofs is considered. The performance of green roofs has been compared to white-coated (reflective) roof surfaces and Sailor et al. [39] concluded that for the majority of building types, the white roof resulted in lower annual energy cost than the baseline green roof, while a densely vegetated green roof was found to outperform the white roof.

For pavement surfaces, however, the performance of highly reflective materials is not as straightforward [34]. In Phoenix, Arizona, brighter surfaces were shown to decrease the canopy air temperature by a maximum of 0.4 °C, but did not result in lower cooling loads [54]. This is due to the fact that increasing the reflectivity of pavement results in higher solar radiation transmitted into the neighboring buildings, which can increase the thermal load or energy use of the building in cooling seasons [54]. It is expected that altering the reflectivity of wall surfaces would similarly affect

the urban energy use, and furthermore have impacts on outdoor thermal comfort.

A few studies have focused on the reflective properties of multiple urban surfaces. For instance, the data measured in the center of Athens proved that increasing the albedo of deep canyon surfaces can lower ambient air temperature up to 1 °C [16]. However, thermal load modifications were not determined as the building energy balance was not considered in these measurements. Simulations for Sacramento, California, indicated that increasing the overall urban albedo of walls and roofs can result in total cooling savings of up to 35% [49], but the contribution of wall albedo compared to roof materials were not identified.

The evaluations of cool (reflective) roofs, green roofs, and cool pavements have contributed greatly to our understanding of the role of surface properties as mitigation strategies. However, it appears that studies considering the effect of high wall albedo in thermal loads and outdoor temperature are limited, motivating an in-depth analysis on the impact of wall albedo in the current study. On the other hand, the majority of studies on the topic only refer to mid-latitudes cities and only a few recent studies have been dedicated to the (sub)tropical regions, where expected population growth and high annual temperatures will increase the impact of urban heating on energy use and comfort. Such analyses represent less than 20% of all climate studies [37]. In Singapore, studies have evaluated ambient air temperature and UHI magnitude using sensor measurements, climatic or satellite-based data [9,31,52], as well as numerical simulation of urban-to-canopy energy balance [5]. Nonetheless, detailed analyses that evaluate mitigation strategies from the standpoint of both indoor (building energy load) and outdoor (UHI and thermal comfort) environments are still lacking and call for further investigations.

Responding to aforementioned gaps in the literature, the aim of this study is to conduct a comprehensive evaluation regarding the effectiveness of reflective (cool) walls on (1) building thermal load, and (2) outdoor temperature and UHI in urban neighborhoods. The city of Singapore with 100% urban population is chosen as the test case in order to enrich the microclimate evaluations in the tropical regions. We study two distinct urban neighborhoods, one residential and one commercial, indicating the bounds of urban density in the studied city as well as demonstrating the intra-urban microclimate variabilities and the impact of urban configuration [35,54,57]. Additionally, it is important to consider the thermal and radiative properties of urban materials, as well as Heat, Ventilating, and Air Conditioning (HVAC) System schedule, which directly impacts thermal loads. Therefore, for achieving a comprehensive evaluation, urban design parameters that modulate the effectiveness of cool walls, such as window solar heat gain coefficient (SHGC) and window-to-wall ratio (WWR), are also taken into consideration. The main objectives are to a) give insight on a potential mitigation strategy of UHI in urban environments, and b) provide an effective metric for cool wall performance that can further inform the development of the cool-wall technologies, such that urban design can effectively contribute to a livable and sustainable city.

The study is structured as follows. Section 2 presents the research methodology, including a validation case followed by a detailed description of the simulation approach. The different simulation cases are defined in Section 2.3. The following questions are then addressed in the results section (Section 4): How are outdoor temperature and indoor energy loads modified by wall albedos? Which design parameters contribute to the impact of wall albedo on the two studied variables, and how? In order to answer these questions, 101 simulation cases cover different characteristics of urban neighborhoods, HVAC schedules, and window properties, each modulating the impact of wall albedo. A discussion of findings is included in Section 5 followed by the conclusion and discussion on future research (Section 6).

2. Methodology

The following section represents the research methodology by describing the numerical approach (Section 2.1), detailing the studied building prototypes and climate zone (Section 2.2), and outlining the simulation cases (Section 2.3).

2.1. Numerical approach: Temperature of urban facets, indoor-outdoor building energy simulator (TUF-IOBES)

Fig. 1 summarizes the methodology workflow and formulations that are used for calculating building energy load and outdoor air temperature.

The main simulation tool used for the assessment of building energy load and outdoor air temperature is the "Temperature of Urban Facets Indoor-Outdoor Building Energy Simulator" developed by Yaghoobian and Kleissl [55] and Krayenhoff and Voogt [23] that dynamically couples the indoor/outdoor energy balances (schematized in dashed green box in Fig. 1). TUF-IOBES is a three-

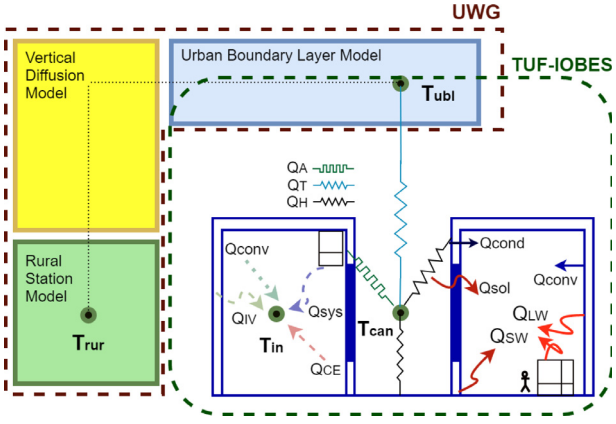

Indoor Air Energy Balance: (1)

$$Q_{conv} + Q_{sys} + Q_{CE} + Q_{IV} = 0$$

Indoor Surface Energy Balance: (2)

$$Q_{conv} + Q_{cond} + Q_{sol} + Q_{LWX} + Q_{LWS} + Q_{SW} = 0$$

Outdoor Air Energy Balance: (3)

$$Q_H + Q_T + Q_A = 0$$

Fig. 1. The diagram of the modeling approach and formulations for obtaining the thermal loads and urban temperatures [5,55]. The (well-mixed) indoor air heat balance (Eq. (1)) consists of convection heat transfer from the zone surfaces to indoor air (Q_{conv}), convective part of internal loads (Q_{CE}), the sensible load due to infiltration and ventilation (Q_{IV}), and the heat transfer to/from the HVAC system (Q_{sys}). The indoor surface energy balance model (Eq. (2)) is based on subroutines in the ASHRAE Toolkit [33], where Q_{LWX} is the net longwave radiant exchange flux between zone surfaces, Q_{SW} is the net shortwave radiation flux to the surface from interior light, Q_{LWS} is the longwave radiation flux from equipment, people, and lights in a zone, Q_{cond} is conduction flux through the wall, and Q_{sol} is the transmitted solar radiation flux absorbed on indoor surfaces. Lastly, canopy air temperature (Eq. (3)) is calculated according to three different terms: the convection from building and ground surfaces (Q_H), the sensible waste heat rejected into the canyon (Q_A) and the sensible heat flux exchanged with the above canopy layer (Q_T).

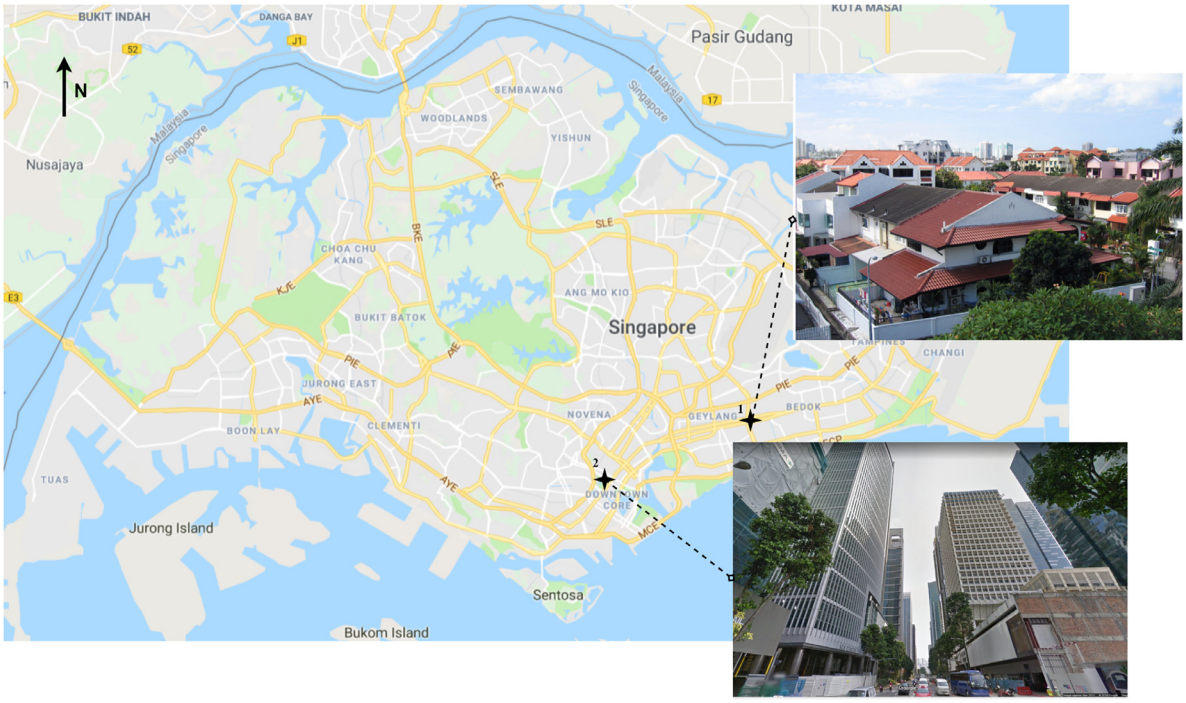

Fig. 2. A map of Singapore (taken from Google maps) with the representative neighborhoods marked. Neighborhood 1 indicates the Telok Kurau district (picture taken from Roth et al. [37]), representative of the low-rise residential neighborhood or LCZ 6, and neighborhood 2 stands for the Central Business District, classified as the high-rise commercial district or LCZ 1.

dimensional building-to-canopy model that intakes (a) meteorological forcing data at the urban boundary layer, (b) building and urban geometry, and (c) thermal and radiative properties of urban materials (detailed in Section 2.2) in order to simulate the (1) detailed 3D outdoor surface temperatures and fluxes, (2) total indoor energy load, and (3) outdoor air temperature in an street canyon, for a non-vegetated and idealized urban configuration.

Unlike the gridded outdoor energy model (detailed in Appendix A) that calculates the distribution of surface temperature on each facade [23,55], the indoor model computes bulk heat exchange and temperature between surfaces and does not specify indoor zones. The building occupancy schedules, HVAC system operation as well as electric and lighting consumption, determine the indoor energy balance to obtain indoor air temperature (T_{in}) and cooling/heating loads inside the building (Eq. (1)). This energy balance is also influenced by conduction through the walls, which impacts convection from walls to room air (Eq. (2)). And lastly, the waste heat from the HVAC system rejected into the street canyon is calculated, which heats the canopy air (Eq. (3)). Canopy air temperature is calculated according to three different terms: convection from building surfaces (Q_H), sensible waste heat rejected into the canyon (Q_A) and sensible heat flux exchanged with the above canopy layer (Q_T). UHI is then calculated based on the difference between the canopy air temperature (T_{can}) and the air temperature in the rural surroundings (T_{rur}).

The meteorological forcing data (T_{ubl}) at a reference height in the TUF-IOBES model comes from the Urban Weather Generator (UWG) [4], demonstrated as the brown dashed box in Fig. 1. The UWG calculates vertical profiles of air temperature from the air temperatures, velocities, and sensible heat fluxes measured at the rural weather station. The urban boundary layer (UBL) model then calculates air temperatures above the urban canopy layer to force the TUF-IOBES model. The urban canopy temperature obtained by the UWG model using the same set of rural data has been previously validated for Singapore [5] and more information regarding the underlying calculations in the UWG model can be found in Bueno et al. [4].

2.2. Local climate zone, building prototypes, and indoor equipment setup

An island state located in South-East Asia (between 1°09′N–1°29′N, and 103°36′E–104°25′E), Singapore was chosen to evaluate the influence of cool walls on thermal loads. With 5.61 million population in 2017, Singapore is a densely populated nation with 100% urban population and a tropical climate with uniformly high temperatures and humidity throughout the year. Accordingly, HVAC systems only provide air conditioning and ventilation, which accounts for about 37% of the total household electricity consumption according to a survey conducted by the National Environmental Agency, Singapore [29].

We selected two distinct urban neighborhoods to represent the range of urban density and therefore the overall range of the mitigation strategies on energy loads and UHI in Singapore: (1) **low-rise residential** neighborhood (such as the Telok Kurau district), and (2) **high-rise commercial** neighborhood (such as the Central Business District). Fig. 2 shows a map of Singapore with these representative neighborhoods marked with photos. According to Stewart and Oke [47], the low-rise residential neighborhood corresponds to local climate zone (LCZ) 6, or open low-rise, and the high-rise commercial district is classified as LCZ 1, or compact high-rise. A 5 × 5 array of idealized buildings is used to represent the geometrical characteristics of the urban neighborhoods. The computational domain vertically extends from the subsurface to the reference height in the canopy layer. Each neighborhood is then represented by a specific building type based on data gathered by previous studies and provided by local government agencies such as the Building and Construction Authority (BCA). Each building has one window per wall, which is analyzed with the fen-

Table 1
Geometrical characteristics of the buildings and street canyon for each neighborhood type, taken from previous investigations in Singapore as referenced.

		Building type	
		Residential	Commercial
Geometrical characteristics	**Local climate zone (LCZ)**	**Open low-rise – LCZ 6** [47]	**Compact high-rise – LCZ 1** [47]
	Canyon width W (m)	**10.0** [9]	**13.3** [9,13]
	Building height H (m)	**10.0** [9]	**80.0** [13]
	Building length L (m)	**16.6** [9,37]	**37.4** [13]
	Total floor area A (m^2)	**275.5**	**1398.8**
	Floor number N (–)	**3** [9]	**20** [13]
	Canyon aspect ratio AR (–)	**1.0** [9]	**6.0** [9]
	Plan area density λ_p (–)	**0.39** [37]	**0.54** [9,13]

Table 2
Angular and diffuse SHGC, absorptance, and transmittance of window glass for SHGC = 0.2. Properties of double pane windows which are used in modern buildings for Singapore are simulated using the WINDOW v7.4.8.0 software and correspond to the product named 'SOLARSTOP Gray' [51]. The window SHGC is then varied by modifying the angular transmittance.

Incident angle	SHGC 0.2	Absorptance (Pane 1 - out)	Absorptance (Pane 2 - in)	Transmittance (SHGC=0.2)
0	0.221	0.681	0.122	0.033
10	0.223	0.686	0.124	0.033
20	0.222	0.690	0.123	0.032
30	0.220	0.690	0.121	0.031
40	0.216	0.684	0.118	0.030
50	0.209	0.675	0.113	0.028
60	0.194	0.659	0.102	0.024
70	0.162	0.608	0.079	0.017
80	0.101	0.439	0.042	0.007
90	0.000	0.000	0.000	0.000
Diffuse	0.198	0.650	0.106	0.026

estration model in TUF-IOBES [55]. Table 1 summarizes the canyon geometry corresponding to each neighborhood.

For the commercial neighborhood, the Singapore office building design is chosen based on the SinBerBEST benchmark model, effective since 2010 [13]. The canyon aspect (height to width) ratio of 6 is typical of the center of commercial and shopping area in Orchard Road [9] and Central Business District (CBD). Table 2 details the window properties followed by Table 3 further describing the thermal and radiative properties of the building components. Windows are selected as double-pane with a separating layer of gas between the two glasses (cf DoublePaneWindow in Duarte et al. [13]). The SHGC of the window is equal to 0.5 and the WWR is set to 45% for the base case, though these factors are varied for further analysis on the effectiveness of cool walls. Unlike the SinBerBEST benchmark model, the composition of exterior walls has been modified to obtain a U-value of 2 W/m^2K, considering that the 0.4 W/m^2K value proposed in Duarte et al. [13] is significantly lower compared to the BCA examples as well as other recent studies in Singapore [6,11]. The semi-rigid insulation material used in SinBerBEST was kept but its thickness was decreased to 10 mm. Note that this value is not physically available but provides the desired U-value of the envelope.

For the residential district, a canyon aspect ratio of 1 and a height of 10 m are chosen based on the low-rise residential neighborhood described in Chow and Roth [9] and Roth et al. [37]. The urban packing density (λ_p) is smaller than for the commercial neighborhood (0.54), and set to 0.39 [37]. In agreement with BCA [6] and Chua and Chou [10], the U-values of windows and walls equal 4.5 W/m^2K and 3.5 W/m^2K, respectively. The semi-rigid insulation thickness was decreased to 3.5 mm. WWR and glazing SHGC are varied throughout the simulations and the remaining thermal properties correspond to the commercial building values. For both building types, street construction is an asphalt layer over one layer of crushed rock [21,26].

The Coefficient of Performance (COP) of the commercial buildings cooling system is chosen as 4.8, consistent with BCA Green Mark for non-residential buildings in Singapore [7] minimum chiller water plant performance for large commercial buildings. COP is 2.5 for the residential district, as similarly suggested in previous studies of residential buildings in Singapore [5,10]. Design loads and schedules of buildings follow the SinBerBEST report and BCA regulation [6,13] and are demonstrated in Fig. 3. Cooling set-points, internal loads for lighting and equipment, people occupancy as well as COP and minimum outdoor airflow required for both building types are summarized in Table 4. Throughout

Table 3
Thickness, thermal properties, and radiative characteristics by layer for building and ground materials in modern Singapore. Properties of the double pane windows are for a product named '1 SOLARSTOP Gray' in the WINDOW v7.4.8.0 software [51]. COM stands for commercial and RES for residential. Unless specified, characteristics are for both building types.

Material layer	Thickness (m)	Conductivity (W.m−1.K−1)	U-value (W.m−2.K−1)	Density (kg.m−3)	Specific heat (kJ.kg−1.K−1)	Solar absorptivity [–]	IR emissivity [–]
Walls (COM/RES)			**2/3.5**				0.9 (inside/outside)
Cement and sand plaster (outside)	0.02	0.533	–	1568	0.991	0.55	–
Concrete	0.15	1.442	–	2400	0.832	0.55	–
semi-rigid insulation (inside) - COM	0.01	0.0335	–	180	0.84	0.7	–
semi-rigid insulation (inside) - RES	0.0035	0.0335	–	180	0.84	0.7	–
Cement and sand plaster	0.02	0.533	–	1568	0.991	0.55	–
Roof			**0.6**				0.9
Cement and sand screed (outside)	0.05	0.533	–	1568	0.991	0.7	–
Expanded polystyrene	0.05	0.035	–	16	1.21	0.7	–
Concrete (inside)	0.2	1.442	–	2400	0.832	0.7	–
Floor			**7.21**				0.9
Concrete	0.2	1.442	–	2400	0.832	0.7	–
Windows (COM/RES)			**2.2/4.5**				
Double-pane							
Glass (SOLARSTOP Gray)	0.0057	1	–	2480	0.7	Table 2	0.84
Argon -COM	0.013	0.016	–	1.78	0.522	–	–
Argon -RES	0.0015	0.016	–	1.78	0.522	–	–
Glass (SOLARSTOP Gray)	0.0057	1	–	2480	0.7	Table 2	0.84

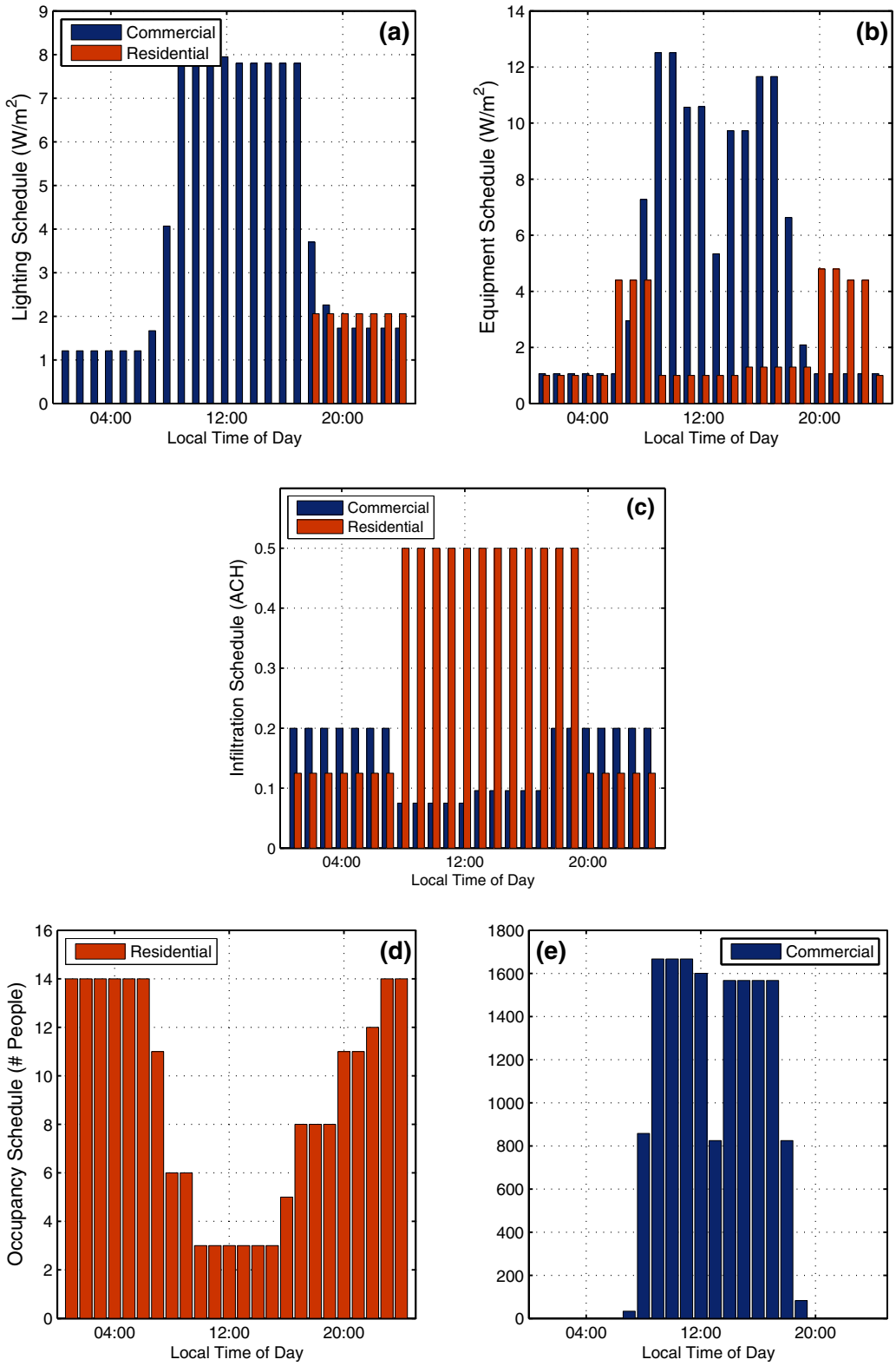

Fig. 3. Schedules and internal design loads: Lighting (a), Equipment (b), Infiltration (c), and Occupancy (d-e) schedules for residential and commercial buildings.

the paper we present cooling loads and not cooling energy use, so the COP is only used when calculating the rejected waste heat.

All HVAC systems work as a dual set-point thermostat with dead-band between minimum and upper set-points. Following Martin et al. [26] and Chua and Chou [10], the maximum set-point for the occupancy-based HVAC schedules (described in Section 2.3) is set to 24 °C. For the continuous operation of HVAC, however, this set-point is increased to 26 °C to lower unnecessary energy consumption in low occupancy periods. The heat transfer from indoor air to HVAC satisfies the air heat balance including the convective heat transfer from the inside zone surfaces, the convec-

Table 4
Characteristics of the indoor building equipment setup taken from previous investigations in Singapore as referenced.

		Building type	
		Residential	Commercial
Equipment parameters	Cooling set-point, continuous (°C)	**26.0**	**26.0**
	Cooling set-point, occupancy-based (°C)	**24.0** [10]	**24.0** [26]
	COP (–)	**2.5** [5,10]	**4.8** (BCA 7)
	Design lighting power density ($W.m^{-2}$)	**2.0** [50]	**12.0** [13]
	Design equipment power density ($W.m^{-2}$)	**5.0** [10,25]	**14.0** [13]
	Occupancy (No. of occupants)	**15** [10]	**2,380** [13]
	Occupant density (m^2/person)	**55.0**	**11.7**
	Infiltration rate (ACH)	**0.5** [5]	**0.2** [13]

tive flux from internal loads and also the sensible load due to infiltration.

Weather data for a representative rural site is from a station at the Seletar reservoir in the central catchment and undeveloped areas in the northwest Singapore, which is considered as the only remaining significant rural area with pockets of tropical rainforest and is primarily used for military training and farming [9].

2.3. Simulation cases

Fig. 4 displays a schematic diagram for the studied cases. The wall albedo (α) is varied between 0.1–0.5, as this range is most representative of the built materials in the urban environment of Singapore. It is found that the impact of wall albedo on thermal loads is linear (i.e. the same impact on thermal loads is seen for every 0.2 change in wall as shown in Fig. 10-a later), and therefore the results of this analysis are presented for $\alpha = 0.1 - 0.3$. Street and roof albedo are set constant to 0.1 and 0.6, respectively.

In the preliminary assessments of this study, it was found that the effect of wall reflectivity on building thermal load highly depends on various building design factors. Therefore, in order to achieve robust analyses on the impact of wall albedo, it is paramount that we consider the contribution of other design elements. In particular, three main factors that contribute to the effectiveness of reflective walls are evaluated here:

1. **Solar heat gain coefficient (SHGC)**: SHGC determines the fraction of incident solar radiation admitted through a window, directly transmitted or absorbed and conducted. Therefore, the variability in SHGC modulates the impact of wall albedo on the thermal load of neighbouring buildings. Wall and ground albedo and diffuse sky radiation determine the incident solar radiation on windows, and SHGC is the critical factor that determines what fraction of that is admitted into the building. To evaluate this factor, SHGC of 0.2, 0.5, and 0.8 are considered here, with detailed window properties summarized in Table 2.
2. **Window-to-wall ratio (WWR)**: WWR, determined by the fraction of the building's gross wall area covered by windows, similarly affects the solar radiation admitted through the building envelope, and therefore interacts with wall albedo through the wall-to-wall radiation exchange in the street canyon. WWR affects admitted solar radiation non-linearly: Raising WWR (i) reduces the reflected radiative energy as the area covered by reflective walls is reduced; and (ii) increases the fraction of wall irradiation that is admitted through the building envelope. Three values of WWR= 0.3, 0.45, and 0.6 are considered here to cover the range commonly seen in Singaporean buildings recorded by BCA.
3. **Heating, ventilation and air-conditioning (HVAC) schedule**: The HVAC schedule directly dominates the building thermal load and the consequent waste heat in the canyon. Three HVAC schedules are considered corresponding to (a) continuous operation (from 00:00 to 24:00), (b) occupancy-based operation from 07:00 to 18:00 for commercial buildings and 22:00 to 07:00 for residential, and (c) no air-conditioning for all hours of the day. Note that no HVAC operation is unrealistic in commercial buildings, therefore schedule (c) is only considered for the residential buildings. An occupancy-based schedule for residential buildings in Singapore is not available in the literature and has therefore been estimated here.

To consider these variabilities together with the impact of wall albedo (Fig. 4), a total of 101 cases are simulated. The simulation corresponds to the first 10 days of April, which includes the warmest days in Singapore and the largest solar elevation angle corresponding to the highest consumption of air-conditioning. The results from the first three days of the simulations are then discarded to remove effects from initial conditions.

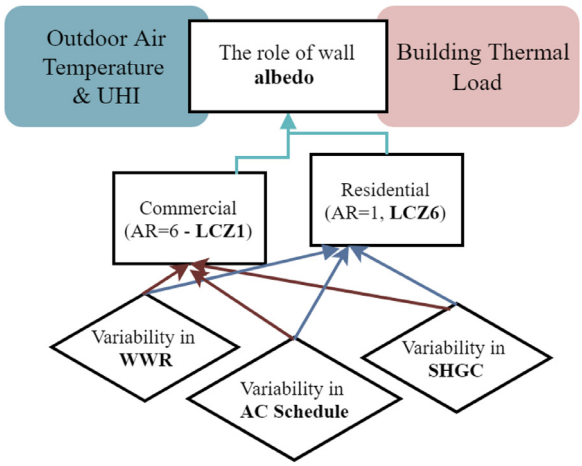

Fig. 4. Schematic of the studied cases on the effect of wall albedo in the context of various urban design parameters.

3. Comparison with UHI measurements in Singapore

In addition to the detailed validation provided for the employed models [5,23,55] described in Appendix A, we compared the simulated results with data gathered in Singapore. Ideally, the performance of the numerical model should be compared against measured thermal load of buildings and UHI. However, such data on building thermal loads in Singaporean neighborhoods are not available to us due to the complexity of required instrumentation in the urban indoor and outdoor environments and/or limitation in access to data. Accordingly, we focus on the UHI value, calculated as the difference between the canopy air temperature in TUF-IOBES and the air temperature at the rural station, and compare the results to a previous study in Singapore by Chow and Roth [9] in Fig. 5.

As UHI is expected to be maximum at night, the results are centered around nighttime, with sunset and sunrise hours identified at 19:00 and 07:00 local time, respectively. The diurnal variation of measured UHI corresponds to the averaged observations between

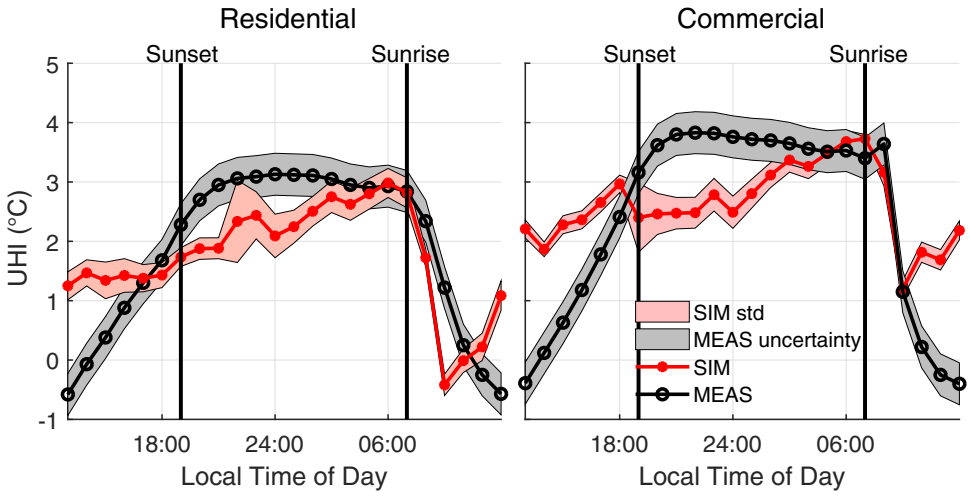

Fig. 5. Comparison of the measured [9] and simulated UHI for residential and commercial neighborhoods in Singapore with continuous operation of the HVAC system throughout the day. The vertical black lines represents the sunset and sunrise hours. SIM stands for simulated and MEAS for measured data. The gray range indicates the uncertainty range of the measurements while the blush pink area corresponds to the standard deviation of UHI in the simulated cases. (For interpretation of the references to color in this figure legend, the reader is referred to the web version of this article.)

March 2003 and March 2004 at the commercial district and between June 2003 and March 2004 at the residential neighborhood [9]. The uncertainty range is situated between ± 0.25 °C for both rural and urban measurements, with the total uncertainty range of ± 0.35 °C for UHI, depicted by the gray area in Fig. 5. The mean diurnal variation of the modeled UHI is depicted in Fig. 5 with red solid lines. As surface materials, WWR, and HVAC schedule are not uniform nor specified in the measurements, the UHI values obtained from the numerical model correspond to the ensemble averaged values for all studied cases described in Section 2.3. Therefore, for each building type, the red line represents the mean and the blush pink area represents the standard deviation of investigated cases over the studied period.

The maximum UHI values simulated here agree well with the measured data for both urban neighborhoods, corresponding to 3.0 °C and 3.7 °C for the residential and commercial areas, respectively. The abrupt decrease in UHI after sunrise is predicted well for both cases. However, the simulated UHI remain below the measured data at night, specifically for the commercial neighborhood. This discrepancy can be attributed to the following factors: (1) The numerical simulations cover a significantly shorter time period compared to the measurements (one week versus one year time-averaging period). A sensitivity study (not shown) demonstrated that the abrupt hourly variations of the simulated data at night are due to this short averaging period and increasing the simulation period to several months flattens the curve. However, in order to perform an extensive parameteric study (101 cases as described in Section 2.3) and considering the low seasonal variability of the climate in Singapore, computational costs forced us to limit the time interval for analyses presented here. (2) The simulations represent an idealized configuration of buildings with uniform characteristics of surface materials and window design. Additionally, the detailed representation of HVAC schedule in the measurements are not available, although it significantly contributes to the UHI in urban environments [24]. For instance, in Section 4.2, we observe that some HVAC schedules result in better agreement with the measured values reported here. Therefore, the lack of data on exact HVAC schedules and the detailed specification of building structures add more uncertainty to the numerical assessment of UHI. 3) Heat exchange overestimation between the canopy and the upper urban boundary layers in the numerical model can further contribute to the discrepancy between the measured and simulated data [15].

4. Results

4.1. Thermal loads

The analysis regarding the impact of wall albedo on thermal loads is done in three steps. First, the thermal loads of the residential and commercial neighborhoods averaged over the studied ranges of SHGC and WWR are compared for various HVAC schedules. Second, we compare the daily variation of cooling load for the two neighborhoods, and this time evaluate the role of wall albedo when two extreme window properties, i.e. small window fraction with small SHGC versus large WWR with large solar heat gain, are considered. Lastly, we compare all the studied cases with variable wall albedos, SHGC, WWR, HVAC schedule, and aspect ratio as well as building characteristics (identified by the two neighborhoods).

4.1.1. Impact of HVAC schedule

Fig. 6 shows the daily variation of cooling load in residential and commercial neighborhoods for continuous and occupancy-based HVAC schedules. The results are averaged for the studied range of SHGC and WWR (Section 2.3), and represented for $\alpha = 0.1$. For continuous HVAC operation, the daily variation of thermal cooling has a bell-shaped curve with a maximum reached after 15:00 local time for both building types, corresponding to high canopy air temperature and solar radiation. For the commercial building, a drop in the cooling load is observed at midday (13:00 local time) corresponding to two factors: first, the occupancy at this hour (shown in Fig. 3-b) is significantly reduced due to the office lunchtime, and second, high solar elevation at solar noon results in a significant decrease in the incident solar radiation on building windows. For the occupancy-based HVAC schedule, the cooling load during the hours of operation is larger since –unlike for continuous operation– the indoor air temperature is not controlled at all times and increases outside the desired range of indoor air temperature. This requires a larger cooling load, especially in the initial hours of operation. Nonetheless, the total thermal load over the entire day, particularly for the residential building, remains lower as increased indoor air temperature reduces conduction heat gains during the day.

4.1.2. Impact of wall albedo considering various window designs

In the second step, the thermal load for the two neighborhoods is compared with variable wall albedos ($\alpha = 0.1, 0.3$) for selected

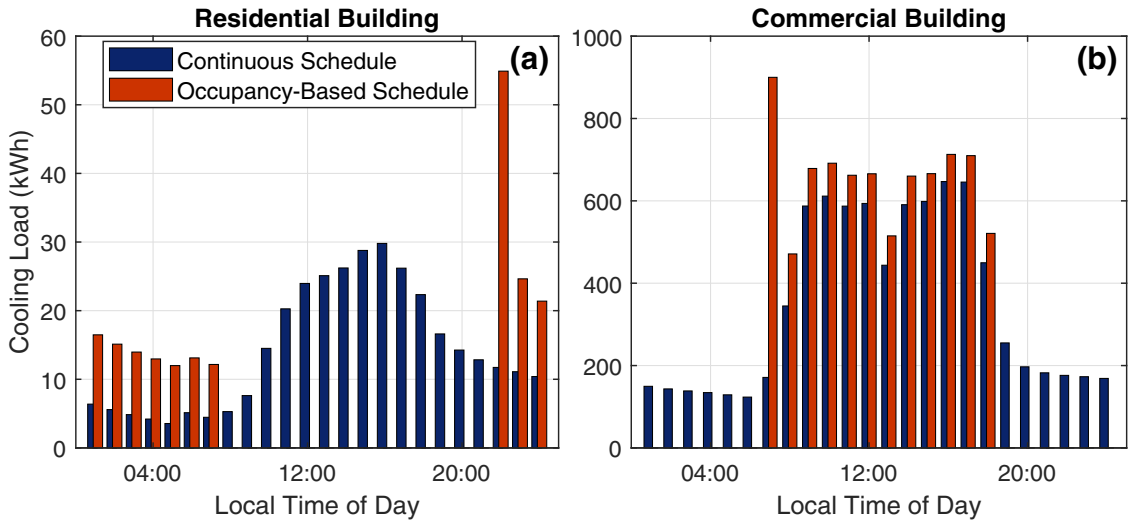

Fig. 6. Daily variation of cooling load in residential and commercial neighborhoods, (a) and (b) respectively, and using two schedules of HVAC operation representing continuous and occupancy-based operation schedules. The results are shown for $\alpha = 0.1$ and averaged for the studied range of SHGC and WWR (Section 2.3).

cases that highlight the range of window properties (Fig. 7). Two sets of SHGC and WWR represent the extreme cases of window properties studied here: (a) large window fraction on all walls with high solar heat gain through the window (WWR = 0.6 and SHGC = 0.8) and (b) a small fraction of walls covered with windows with small solar heat gain (WWR = 0.3 and SHGC = 0.2). Two main observations are made. First, the impact of wall albedo is small compared to the role of window properties, specifically in the residential neighborhood (lower aspect ratio) and for continuous operation (Fig. 7-a). For the occupancy-based operation in the residential neighborhood (Fig. 7-c), on the other hand, the role of window properties is much smaller and the higher wall albedo always reduces cooling load since the lower heat storage and heat conduction through walls dominates at night time. Nonetheless, the impact of wall albedo is small and limited to a maximum of 1 kWh for $\Delta\alpha = 0.2$ (Fig. 7-e). Second, it can be seen that the higher wall albedo results in a higher value of thermal load for the commercial building (Fig. 7-b/-d/-f), which is counter-intuitive to the expectation of higher wall albedo reducing lower thermal load. In order to fully grasp these observations, it is important to consider a few factors:

a) The variability in the **canyon aspect ratio** is a critical factor in the building thermal load as the interactions between buildings are significantly increased when they are positioned closer to each other. The canyon aspect ratio determines inter-building shadowing that reduces solar radiation incident on walls and the wall-to-wall view factors associated with longwave radiation exchange between buildings.
b) Several heat transfer mechanisms (Fig. 1 and Eqs. (1)–(3)) determine the overall thermal load of the building, and among those, two main mechanisms are affected by the wall albedo. First, the **(conduction) heat transfer through the wall (Q_{cond})** is modified. The albedo of the outer wall determines the solar radiation absorbed by the surface, which further determines the outdoor surface temperature. Accordingly, when evaluating the indoor surface energy balance (Eq. (2)), the conduction through the wall is modified as it is directly correlated with the difference of indoor and outdoor surface temperatures. Second, the **(transmitted) heat transfer through the windows (Q_{sol})** is affected. The wall albedo determines the reflected solar radiation from the walls, and consequently, the portion that is transmitted into neighboring buildings. Window transmission of wall-reflected radiation is more pronounced for higher canyon aspect ratios with increased wall-to-wall view factor (note a). The transmitted solar radiation directly affects the indoor surface temperature and modifies the convective heat flux from the surface (Q_{conv} in Fig. 8 and Eq. (1)), altering the building thermal load. The radiative energy reflected by walls and transmitted through windows increases linearly with wall albedo and window transmissivity.
c) **Window properties (window-to-wall fraction and solar heat gain)** contribute to the indoor surface and air energy balance. Without windows, the effect of wall albedo on thermal load is confined to the change in indoor surface temperature through the wall conduction. In the presence of windows, however, the balance between the Q_{cond} and Q_{sol} is dominated by the window properties. The radiative energy transmitted through windows increases linearly with window transmissivity, window-to-wall ratio, and incident irradiance (direct from sun, diffuse from sky, and reflected from urban surfaces).
d) While window transmission is immediate, wall conduction delays heat transfer. Therefore window properties affect thermal load primarily during the day, while wall conduction changes with albedo affect thermal load most strongly in the evening.

The overall thermal load is determined by a combination of these factors. In the case of high aspect ratio (i.e. significant interaction between urban facades) and high WWR and SHGC (i.e. increased transmitted solar radiation into the building), the increase in wall albedo results in increased window transmittance. The impact of the decreased outdoor wall surface temperature, on the other hand, is delayed due to wall heat storage. Accordingly, the increased wall albedo demands more cooling energy to offset the increased convection from indoor surfaces (Fig. 8).

In Fig. 9, we calculate the total annual cooling load per gross floor area, assuming that the daily thermal load is identical to Fig. 7 for the entire year. This is acceptable for the tropical climate of Singapore where the inter-seasonal variability in the air temperature is very small. Although the absolute thermal cooling in kWh is significantly higher for the commercial building (Fig. 7), the annual cooling load per floor area (kWh/m^2/year) in Fig. 9 is larger for the residential building. This is similarly seen in the 2003 CBECS Survey data for USA [14] that demonstrated that Energy Use Intensity, and similarly the thermal load, does not vary monotonically with the gross floor area.

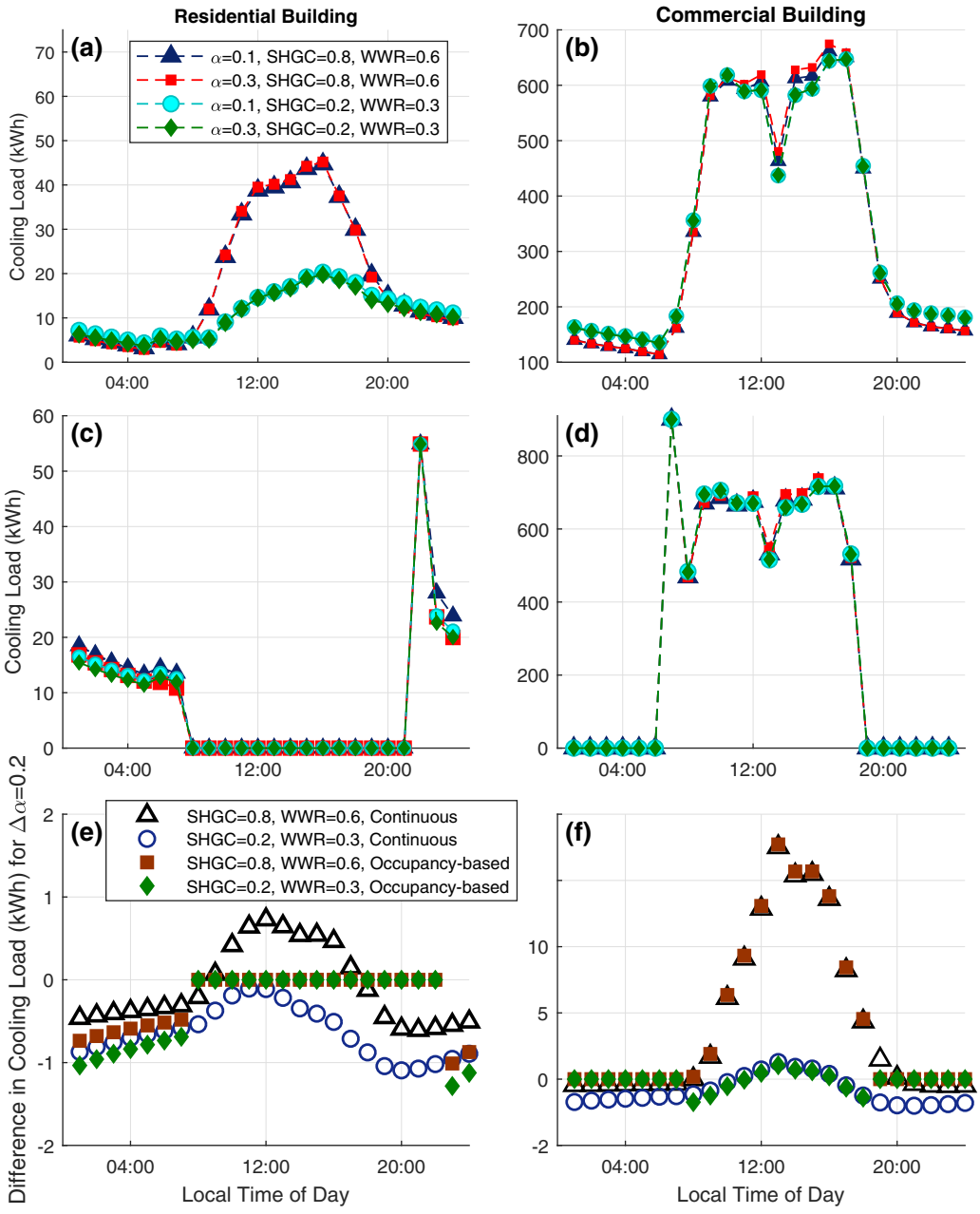

Fig. 7. The daily variation of cooling load in residential and commercial neighborhoods, (a,c,e) and (b,d,f) respectively. Plots (a,b) and (c,d) demonstrate the daily variation of cooling load for continuous and occupancy-based operation of HVAC, respectively, while (e,f) demonstrate the cooling load difference (in kWh) when wall albedo is varied by 0.2 ($\Delta\alpha = 0.2$). The results are shown for four selected cases with two sets of SHGC and WWR and two values of wall albedo. Note the different limits of the y-axes.

A few observations are made from Fig. 9. First, for the residential building, the importance of the HVAC schedule is highlighted. The highest air temperature during the day corresponds to the lowest occupancy level in the residential buildings, and therefore, a significant reduction in the thermal load can be achieved if the HVAC schedule is adjusted accordingly. Second, in the case of the continuous operation, the role of the window properties become significant, and more important than the wall albedo. The reduction in thermal load by using better thermal properties and smaller windows cuts the thermal load approximately in half, while a wall albedo increase of 0.2 reduces cooling load only by 6.5%. This trend is less-pronounced when the occupancy-based AC schedule is used: the window modifications contribute to 3–8% reduction in cooling load (comparing cases with the solid black and dashed yellow borderline in Fig. 9), while the wall albedo reduces cooling load by 4–10%. However, it is worth noting that in the case of existing developments, modifying wall albedo is more economical than altering window properties, and therefore is a more practical solution for reducing thermal load. Lastly, we observe that for the commercial buildings, the trends are different. As described before, increased wall albedo results in higher cooling load due to the large canyon aspect ratio when the window-to-wall fraction and solar heat gain coefficients are large. Additionally, the role of the HVAC schedule is not as significant as in the residential buildings.

4.1.3. Comprehensive sensitivity analysis

In the last step of this analysis, we compare the daily average cooling load for all studied cases (Fig. 10). The following observations are made:

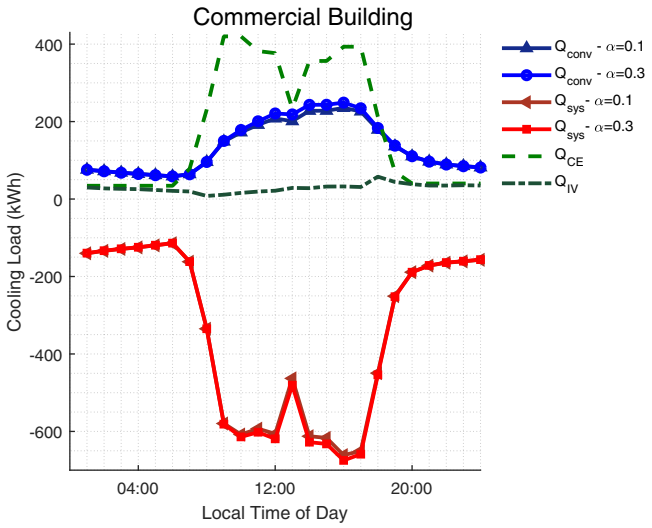

Fig. 8. The daily variation of indoor air energy balance components (Eq. (1)), which consists of convection heat transfer from the zone surfaces to indoor air (Q_{conv}), convective part of internal loads (Q_{CE}), the sensible load due to infiltration and ventilation (Q_{IV}), and the heat transfer to/from the HVAC system (Q_{sys}). The plots are shown for SHGC = 0.8 and WWR = 0.6.

a) The cooling load increases with increasing SHGC for both building types and HVAC schedules and significant majority of WWR.
b) In the residential building (lower aspect ratio) with continuous HVAC operation (Fig. 10-a), the cooling load increases with increasing WWR and SHGC. This is due to the fact that the lower aspect ratio results in more direct and diffuse sky solar radiation density incident on the building facades during the day compared to the commercial building, which is directly transmitted into the building through the windows (Q_{sol} in Eq. (2)). Therefore, the larger the windows, the more solar radiation is transmitted into the building, and if the HVAC is operating during these hours, the higher is the cooling demand. The increase in wall albedo then reduces the residential cooling load, specifically when the windows have a smaller solar heat gain (i.e. avoiding the reflected radiation to be transmitted through the building) due to the decreased outdoor surface temperature.
c) Except for the residential building with continuous operation of HVAC, the relationship between the cooling load and WWR is not monotonic. This is due to the fact that the WWR modifies the cooling load in two different ways: (1) conductive heat transfer is modified as the U-value of window and wall surfaces are different, with walls often being more insulated (here wall and window U-values are 2 and 2.2, for commercial buildings, and 3.5 and 4.5 for residential buildings, respectively), and (2) transmitted solar radiation is modified due to the change in cumulative radiative energy across the total window area. In the common case of lower U-value for windows (Table 3), the two mechanisms have a counteracting effect on the building cooling load. These factors are also significantly modified by the canyon aspect ratio: higher aspect ratio results in larger inter-building shadowing, decreasing both window transmitted radiation and conductive heat transfer to the building. Due to these counteracting effects, we observed that increasing WWR in the commercial neighborhood (AR = 6) results in a decrease in thermal load. Specifically, when the continuous operation is considered, the conductive heat losses at night (when the transmitted solar radiation is absent and windows radiate against the cold sky) dominate over transmitted solar radiation and cooling load decreases with WWR. Note that although conduction and transmitted radiation are modified by both wall albedo and WWR in the heat balance equation (Eq. (2)), the ways in which albedo alter these mechanisms are different. When albedo is modified, conduction is altered based on outside surface temperature and transmitted radiation is modified due to the reflected solar radiation.
d) The impact of wall albedo on cooling load foremost depends on building type and canyon aspect ratio, followed by the window properties. For the residential neighborhood with a lower canyon aspect ratio (AR = 1), the increase in wall albedo persistently decreases the cooling load and is most significant when SHGC is low. For the commercial neighborhood with a significantly larger aspect ratio (AR = 6), however, there is a cross point where the role of wall albedo becomes reversed. For both occupancy-based and continuous operation, it can be seen that for low solar heat gain (SHGC = 0.2), increasing wall albedo reduces cooling load. When the SHGC is increased to 0.5, however, the WWR determines the impact of wall albedo, and after SHGC is further increased to 0.8, the larger wall albedo increases the thermal cooling for all WWR values. Therefore, we observe that for the commercial neighborhood, the transmitted solar radiation dominates the reduced net wall conduction when SHGC > 0.5, increasing the thermal load with increased wall albedo.

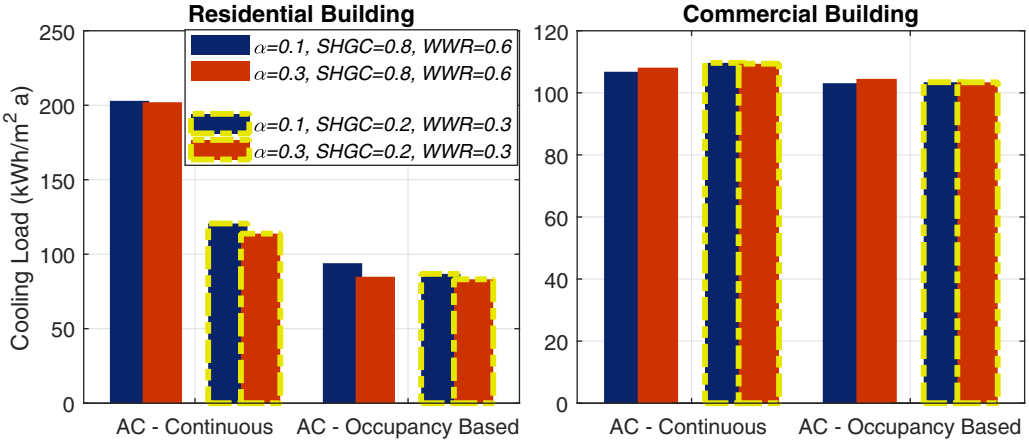

Fig. 9. Extrapolated total annual thermal load per gross floor area (kWh/m^2 year) for residential and commercial neighborhoods with various HVAC schedules. Bar charts with yellow borders represent the cases with the lowest fraction of window areas and smallest solar heat gain considered (SHGC = 0.2 and WWR = 0.3), while colors represent the wall albedo. (For interpretation of the references to color in this figure legend, the reader is referred to the web version of this article.)

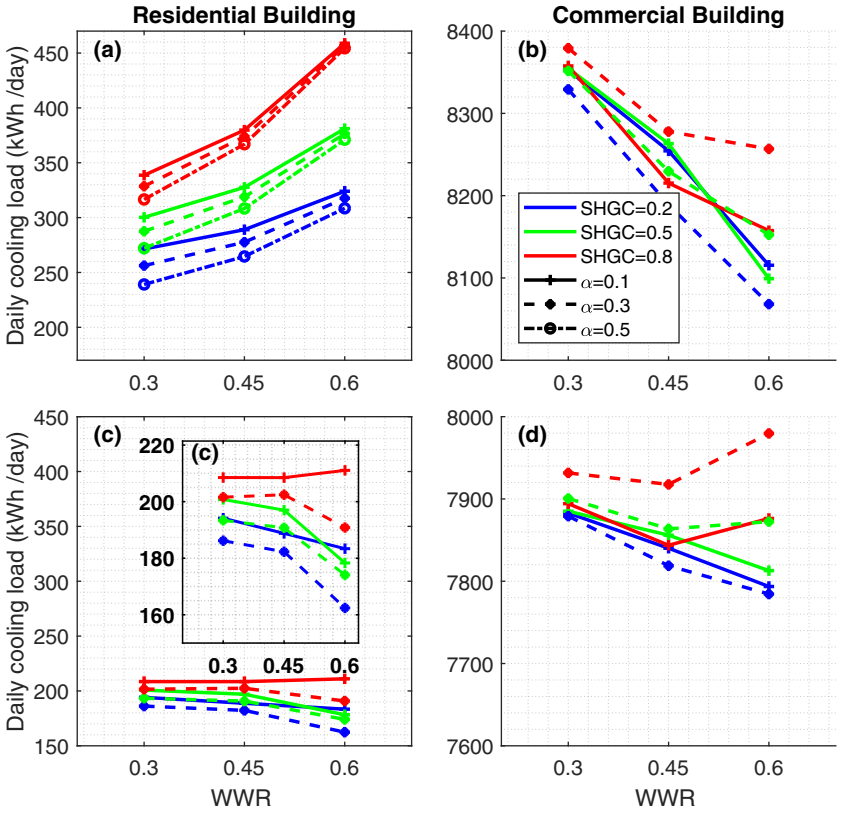

Fig. 10. Sensitivity study regarding the effects of wall albedo on total daily cooling loads in Singapore neighborhoods. Plots (a,b) represent continuous operation (00:00–24:00) and (c,d) indicate occupancy-based operation with daytime HVAC for commercial buildings and nighttime operation hours for residential.

4.2. Outdoor air temperature and urban heat island

The analysis regarding the impact of wall albedo on outdoor air temperature and UHI is done in two parts. First, the daily variation of UHI in the residential and commercial neighborhoods is compared for various HVAC schedules and the change in UHI for $\Delta\alpha = 0.2$ is evaluated. Second, we compare the daily mean and maximum values of UHI for all the studied cases with variable wall albedos, SHGC, WWR, HVAC schedule, and aspect ratio as well as building characteristics (identified by the two neighborhoods).

4.2.1. Impact of wall albedo considering various HVAC schedules

Fig. 11 demonstrates the daily variability of canopy air temperature (T_{can}) and UHI for the commercial and residential neighborhoods for different HVAC schedules. The simulations are presented for SHGC = 0.2 and WWR = 0.3, while the wall albedo is varied. This case yields the largest wall albedo reduction in cooling load and is also expected to yield the largest UHI reduction as net wall surface area is maximized.

For the residential neighborhood, the scenario with no-HVAC operation minimizes UHI throughout the day, with the maximum at 2.7 °C reached before sunrise. When the HVAC operation is adjusted to the occupancy of the residential building (operation from 22:00 to 07:00 local time), we observe a reduction in UHI during the day compared to continuous HVAC operation, but a significant increase (max UHI reaching 3.4 °C) at night when the HVAC is in operation. This value is higher than the UHI calculated for the case with continuous HVAC operation, as the thermal load at night hours is higher in the occupancy-based schedule (Fig. 6). For the commercial neighborhood, however, since the occupancy-based operation results in lower thermal load at night, the UHI values are also reduced (up to 1 °C at some studied hours) compared to continuous HVAC operation.

The role of HVAC schedule and local climate zone is significantly more pronounced than the wall albedo. While the impact of wall albedo is limited to 0.1 °C (Fig. 11-c/d), the largest difference in peak UHI reaches more than 1 °C between the cases with occupancy-based operation of HVAC and AC-Off for the residential building. This observation is in agreement with the mesoscale simulations by Li and Norford [24] that reported 0.9–1.2 °C UHI reduction in Singapore when no anthropogenic heat was released from buildings. The daily variation of UHI with the (more realistic) occupancy-based operation for the residential building exhibits a closer agreement with the measured data reported in Section 3.

4.2.2. Comprehensive sensitivity analysis

Here, we compare all studied cases and further demonstrate the role of wall albedo on outdoor air temperature in the context of design parameters such as building prototype, canyon aspect ration, HVAC schedules, and window properties. Although the daily mean UHI is a critical factor for assessing urban heating, the maximum air temperature in the urban street canyon should also be represented as it significantly affects the thermal comfort and heat stress of individuals in urban environments. Accordingly, we represent both parameters, i.e. the daily average of UHI and maximum value of T_{can} (Figs. 12 and 13, respectively). We observe the following:

a) Of the three heat transfer mechanisms that determine the outdoor air energy balance (Fig. 1 and Eq. (3)), two are dynamically affected by the design parameters (such as canyon aspect ratio, window properties, and albedo) and building schedules. First, the **convective heat transfer from the building surfaces** (Q_H) is modified due to the change in outdoor surface temperature. Second, the **rejected waste heat into the canyon** (Q_A) is mod-

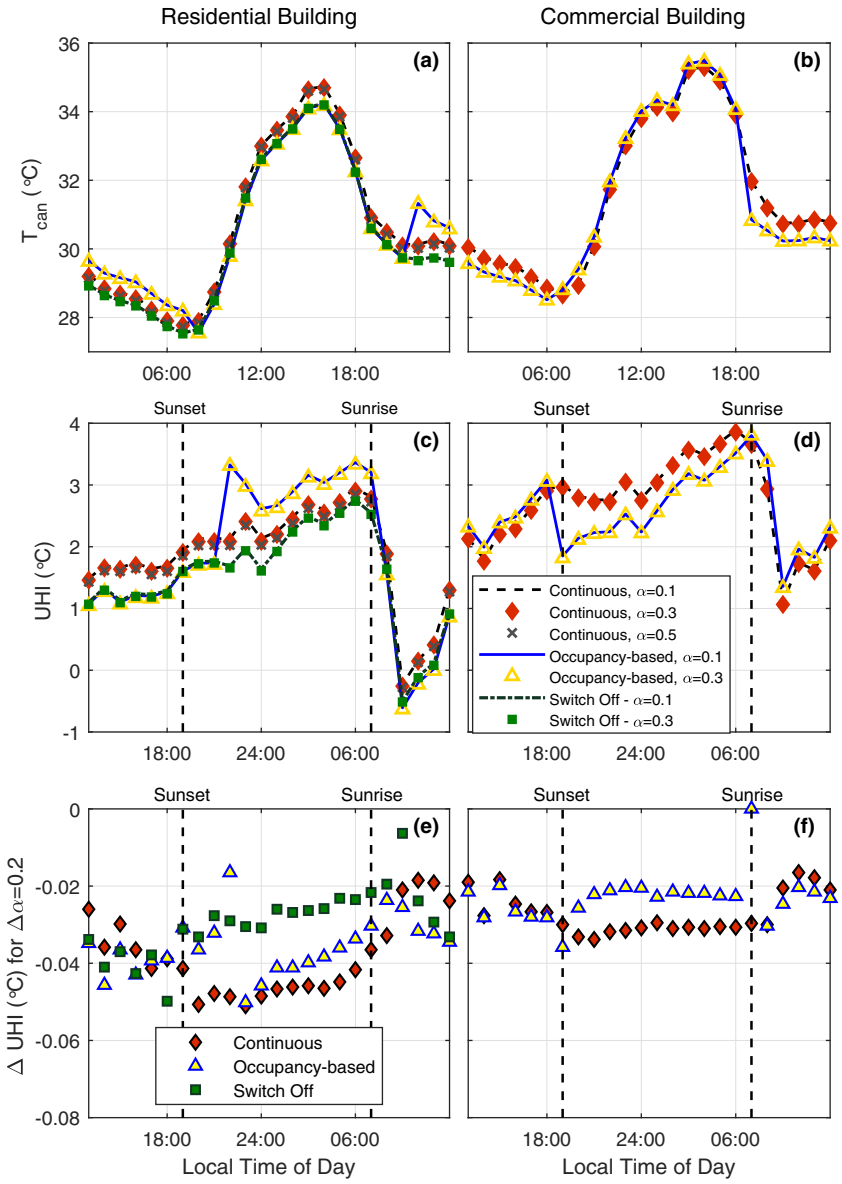

Fig. 11. Daily variation of canopy air temperature (T_{can}) and UHI for commercial and residential neighborhood as a function of HVAC operation schedules and wall albedo (plots (a)-(d)), and the difference in UHI for 0.2 change in wall albedo ($\Delta\alpha = 0.2$) for residential and commercial neighborhoods (plot (c) and (d), respectively). Similar to Fig 5, the UHI is centered around midnight. 'Continuous', 'Occupancy-based', and 'Switch Off' represent the HVAC schedules considered.

ified by the building thermal load. Accordingly, the variability in the thermal load (Fig. 10) is reflected in the change in UHI in some scenarios, while being significantly different for others due to the combined and potentially counteracting effects of these factors.

b) The canyon aspect ratio and building type determine the range and variability of mean UHI and maximum T_{can}. Accordingly, the UHI value is consistently higher for the commercial neighborhood and less sensitive to other design parameters (including wall albedo) considered here.

c) A sensitivity to the HVAC schedule for the residential building is the most dominant factor for the daily mean UHI. When the HVAC is turned off for the entire day, the mean UHI and maximum T_{can} drop to $\sim$1.5°C which is $\sim$0.5°C lower than for the other HVAC schedules.

d) The maximum T_{can} is observed in the commercial building for the cases with occupancy-based HVAC operation (35.5 °C) while the daily mean UHI peaks when the HVAC is in full operation during the day (2.75 °C). This demonstrates the difference in reducing the UHI magnitude versus decreasing the thermal stress concerns in the hot climate.

e) Increased wall albedo reduces daily mean UHI, regardless of building type, window properties, and HVAC schedule. However, this contribution is rather marginal: a maximum reduction of 0.11 °C is observed when albedo is changed from 0.1 to 0.5 for the residential neighborhood with WWR=0.3 and continuous operation.

f) When the HVAC system is used, higher SHGC results in higher daily mean UHI due to the increased anthropogenic waste heat from the buildings (increased thermal load observed in Fig. 10). However, when the HVAC system is turned off, the trend reverses (Fig. 12-e). Higher SHGC results in more heat being admitted into buildings versus into the urban canyon, and therefore UHI is decreased. Nonetheless, the effect of SHGC in mod-

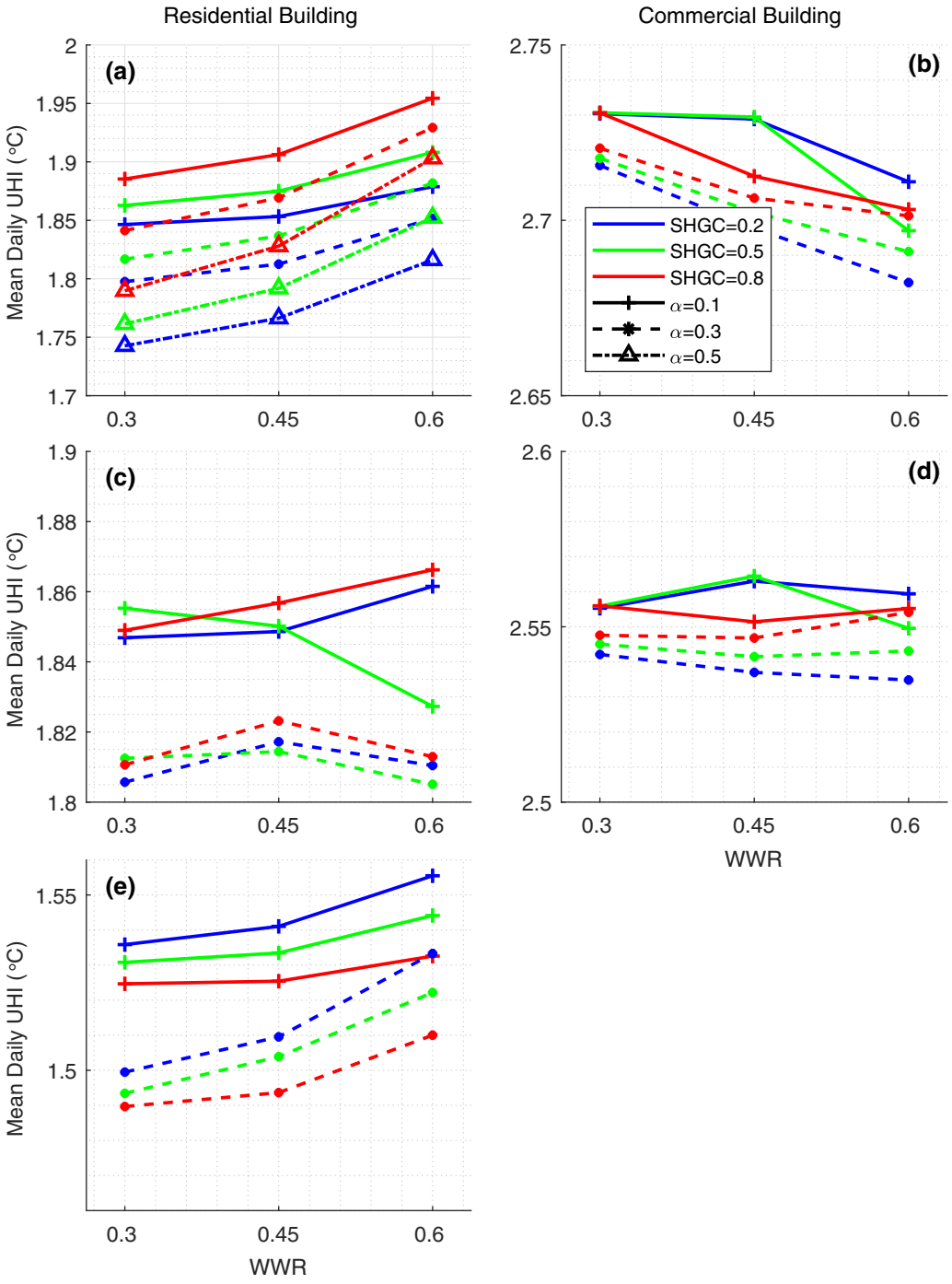

Fig. 12. Sensitivity of mean UHI to wall albedo with varying WWR and SHGC. Values are expressed as a average value for an entire day. The rows correspond to different HVAC schedules, where (a,b) represent continuous operation (00:00–24:00), (c,d) indicate occupancy-based operation with daytime HVAC for commercial buildings and nighttime operation hours for residential, and (e) represents no HVAC operation. Note the different limits of the y-axes.

ifying the UHI values (mean and maximum) is small. Similarly in the residential neighborhood, increasing WWR increases the mean UHI value due to increased outdoor wall temperature during the day (not shown).

g) Maximum T_{can} trends can be different from mean UHI trends, considering that the maximum canopy temperature occurs during the day and therefore, depends on the HVAC operation at that hour. Nonetheless, similar to the analysis of mean UHI, we observe that the role of building design parameters (wall albedo and window properties) on the maximum T_{can} is small compared to the canyon aspect ratio, building type, and HVAC schedules.

5. Discussion

5.1. Thermal load

Table 5 presents a qualitative summary of the impact of various parameters on the thermal (cooling) load. Among the studied parameters, only SHGC results in a monotonic change in the thermal load, i.e. the increase in SHGC results in the increased thermal

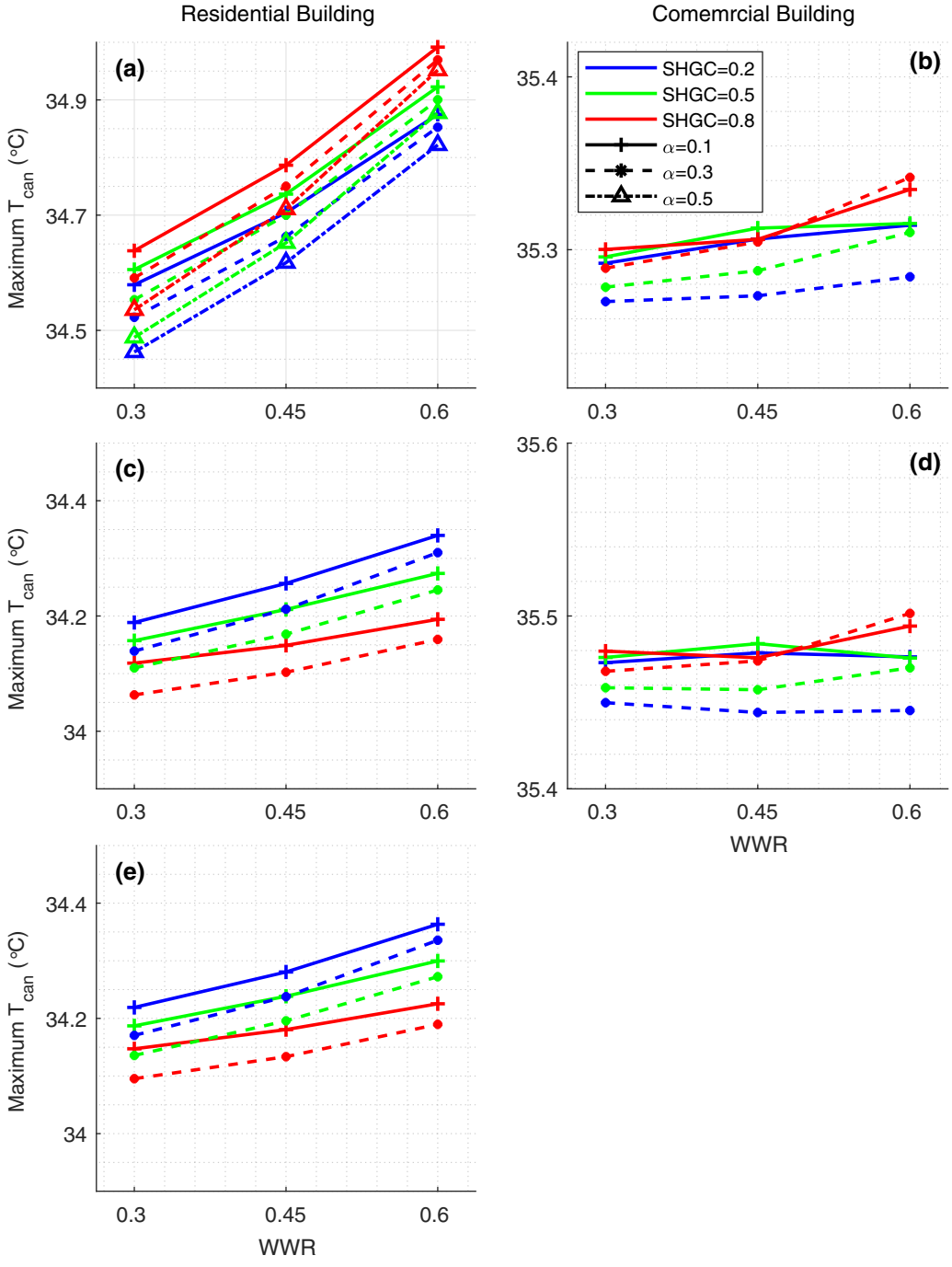

Fig. 13. Similar to Fig. 12 for the maximum T_{can} value for an entire day.

Table 5
Qualitative summary of the impact of different building variables on thermal loads. Arrows indicate the increase (↗) and decrease (↘) in building thermal load as a response to variables such as wall albedo (α), SHGC, and WWR in different neighborhoods and HVAC schedules. Question marks (?) indicate the lack of monotonic trend.

Building type	Residential	Commercial	Residential	Commercial
HVAC schedule	Continuous		Occupancy-based	
SHGC ↗	↗	↗	↗	↗
α ↗	↘	$?^{I}$	↘	$?^{I}$
WWR↗	↗	$?^{II}$	$?^{II}$	$?^{II}$

Table 6
Quantitative summary of the impact of wall albedo on thermal loads. The results are categorized based on the building type and HVAC operation schedule. The average daily cooling load represents the average value of all studied cases in each category (covering cases with variable WWR, SHGC, and wall albedo) and the standard deviation (in kWh and %) indicates the departure from the mean value considering all cases. The effect of wall albedo is divided into "positive" and "negative" impacts, indicating the decrease and increase in cooling load, respectively, as the two trends were observed in Section 4.1.

Building type	Residential	Commercial	Residential	Commercial
HVAC schedule	Continuous		Occupancy-based	
Average daily cooling load (kWh)	13.8	343.5	8.0	327.8
Standard deviation (% deviation)	2.5 (18%)	8.8 (2.5%)	0.5 (5.6%)	4.1 (1.3%)
Min/mean/max "positive" impact of $\Delta\alpha = 0.2$**(%)**	0.1/0.4/0.7	1.0/1.6/3	0.2/0.4/1.1	0.2/0.6/1.0
Min/mean/max "negative" impact of $\Delta\alpha = 0.2$**(%)**	–	0.7/2.5/4.5	–	0.3/1.9/4.1

Table 7
Qualitative summary of different urban variables impact on mean UHI. The arrows indicate the increase or decrease in each parameters.

Building type	Residential	Commercial	Residential	Commercial	Residential
HVAC schedule	Continuous		Occupancy-based		Off
SHGC ↗	↗	$?^{I}$	$?^{I}$	$?^{I}$	$\searrow^{II}$
WWR ↗	$\nearrow^{III}$	↘	$?^{III}$	$?^{IV}$	$\nearrow^{III}$
α ↗	↘	↘	↘	↘	↘

Table 8
Quantitative summary of the impact of wall albedo on UHI (symbols and definitions Similar to Table 6).

Building type	Residential	Commercial	Residential	Commercial	Residential
HVAC schedule	Continuous		Occupancy-based		Off
Average daily UHI (°C)	1.81	2.70	1.85	2.55	1.52
Standard deviation (°C)	0.06	0.02	0.04	0.01	0.03
Min/mean/max impact of $\Delta\alpha = 0.2$ (°C)	0.03/0.04/0.05	0.0/0.02/0.04	0.02/0.03/0.05	0.0/0.02/0.04	0.02/0.03/0.04

load for all studied conditions. When wall albedo and WWR are varied, due to the interdependence of heat transfer mechanisms (Section 4.1), the impact on the thermal load depends on several factors. Increased wall albedo reduces the thermal load in the residential building, but not necessarily in the commercial neighborhood where buildings are placed closer to each other and more reflected radiation enters the adjacent building (I in Table 5). Therefore, depending on the window properties, increasing wall albedo can increase cooling load. Similarly for the WWR, except for the residential building with continuous HVAC operation, the thermal load varies non-monotonically with WWR, which is due to the counteracting effect of conductive heat transfer and transmitted solar radiation throughout the day (II in Table 5). In short, if the walls are shaded (due to higher aspect ratio) and transmissivity is small, thermal load is lower for the buildings with higher WWR.

In Table 6, we summarize the impact of wall albedo on the thermal load for two different building types and two HVAC schedules. The role of wall albedo on mean cooling load is smaller than other studied parameters such as canyon aspect ratio and building type, HVAC schedule, and window properties. For residential buildings, the modification of window properties may in fact yield a more desirable outcome than wall albedo. However, modification of WWR typically is not economically feasible post-construction while the wall albedo can be altered for existing developments, making it a more feasible retrofit mitigation strategy. Lastly, the negative impact of the increased wall albedo in the commercial neighborhood can be larger than the positive outcome, suggesting that high albedo walls should be avoided in densely-built neighborhoods with larger aspect ratio.

5.2. Outdoor air urban heat island

Similar to the analysis of thermal load, we present a qualitative and quantitative summary of the results regarding the UHI variability here (Tables 7 and 8, respectively).

Unlike for building thermal loads, the impact of wall albedo on the canyon air temperature UHI is consistent: higher wall albedo results in lower UHI in the urban canyon for all building types and HVAC schedules. However, the role of SHGC on UHI is more complex. In residential buildings with HVAC operation, the higher SHGC results in higher UHI due to the increased cooling load, and therefore increased anthropogenic heat from the building. When the HVAC is turned off, however, the increase in SHGC reduces UHI (II in Table 7). Similarly for the commercial building, SHGC results in counteracting effects on UHI (reduced convection of heat from wall surfaces into the canyon while increased rejected waste heat), and therefore the trend is non-monotonic (I in Table 7). Lastly, larger WWR results in an increased UHI in the residential buildings due to the increased cooling load and since the outdoor surface temperature of windows is larger than walls during the day, increasing convective heat transfer (III in Table 7). However, this trend is not seen for the commercial building where the surfaces are more shaded and the thermal load contribution is more significant (IV in Table 7). Nonetheless, comparing the quantitative contribution of these parameters (Table 8), the role of wall albedo together with the window properties is smaller than the impact of canyon aspect ratio, building type, and HVAC schedules.

6. Conclusions and future research

The urban overheating can be detrimental to the environment and the quality of life for urban dwellers, particularly during the cooling seasons. While some impacts may be beneficial (including reduced thermal load in winter or lengthening the plant-growing season), the majority of ensuing effects such as increased energy consumption, elevated air pollution, compromised human health and comfort, and worsened lake and river water quality, are deemed negative and deserve attention. To respond to these pressing challenges, it is paramount that various mitigation scenarios are evaluated comprehensively, considering the counteracting ef-

fects of various design and climatic factors. The presented work is an example of such analysis which focuses on cool (reflective) walls as a mitigation scenario in a tropical environment.

We examined the potentials of cool walls as a mitigation strategy for urban heat and means of reducing the building energy use. To achieve a comprehensive analysis, we integrated the perspective of both indoor and outdoor environments and further evaluated the role of various design parameters in modulating the impact of wall albedo. Although the energy saving potentials and air quality benefits of cool roofs, green roofs, and cool pavements have been rigorously evaluated for various climates, to date there has been no detailed evaluation of cool walls, particularly in tropical climates.

Unlike the analysis of cool roofs as a UHI mitigation strategy, we found that a universal conclusion regarding the effectiveness of cool walls cannot be achieved, since the role of wall albedo significantly depends on the urban morphology, building design, and human interaction with buildings (such as occupancy, HVAC schedules, and other contributing factors to anthropogenic heats). Among these factors, local climate zone (dominated by urban density) and building operation dominate the range and variability of building thermal loads and UHI, while window properties modulate the indoor-outdoor heat/radiation exchange. Compared to these factors, the impact of wall albedo is small or and can even be undesirable at times. Nonetheless, in contrast to altering the urban morphology or building design in existing urban areas, the modification of wall albedo represent a more (financially and practically) feasible strategy and can be beneficial depending on the cumulative design of the urban environment. Accordingly, the role of wall albedo should be rigorously evaluated on a case-by-case basis and the presented study demonstrates a detailed methodology of achieving such analysis. Additionally, we note the need for separating the mitigation of UHI that often prevails at night, from the enhancement of thermal comfort in the street canyon which is more concerning during the daytime in the cooling seasons.

The current study demonstrates a comprehensive evaluation of cool walls as a mitigation strategy by representing both indoor and outdoor environments, considering the interdependence of various design and climatic factors, and emphasizing the need for climate-conscious urban design. However, similar to other numerical analyses, limitations persist, which calls for future research:

1. The accuracy of any numerical analysis highly depends on the accuracy of inputs and assumptions. However, the access to detailed and realistic urban data is often limited due to the complexity of microclimate analysis in realistic neighborhoods. For instance, the detailed HVAC schedule based on the various functionality of the buildings was not available/accessible for Singapore, which calls for further detailed assessments. Additionally, considering the state-of-the-art in the numerical modeling of urban physics and the limitations of computational resources, the simulations are bound to a series of assumptions and simplifications. Here, due to the limitation of the numerical model to consider non-rectangular and heterogeneous geometries, only an idealized urban configuration was considered. Similarly, the potential co-benefits of cool walls on lighting energy use were ignored due to the limitation of the numerical model in calculating the dynamic lighting schedule. Therefore, this analysis should be expanded to more realistic geometries and dynamic schedules such that it can inform the design decisions in both cases of already existing urban areas or new urban developments. Simulating a real urban neighborhood depends on the availability of detailed 3D models of buildings as well as the ability of models to simulate realistic configurations. Therefore, further research is needed to not only enhance the numerical models of urban energy to consider the realistic configurations, but also to enhance the accessibility of obtaining such microclimate or geometrical data in urban neighborhoods.
2. Although urban canopy temperature affects human sensation of the thermal environment, thermal comfort is also determined by a range of other factors. Accordingly, for a more comprehensive evaluation, the analysis presented here should be complemented with a detailed evaluation of mean radiant temperature and wind speed in urban streets.
3. This study represents the evaluation of cool walls in a tropical climate of Singapore and should be expanded to include other climatic variations, particularly considering that seasonal variability is expected to modulate the impact of wall albedo.

Acknowledgment

Funding was received from the National Research Foundation Singapore under its Campus for Research Excellence and Technological Enterprise programme.

Appendix A. Supplementary information on the numerical model TUF-IOBES

The TUF-IOBES outdoor energy balance model that determines outside surface temperatures is built upon TUF3D [23], which includes a detailed calculation of view factors and sunlit-shaded algorithms for simulating radiation distribution over a 3-dimensional (3D) domain (demonstrated in Fig. A.14). The geometry of TUF-IOBES is composed of arrays of buildings while outdoor surfaces are subdivided into patches (grids) of identical size. The outdoor surface energy balance, consisting of net longwave and shortwave radiation (accounting for multiple reflections), conduction, and convection, is then solved and enforced for each outdoor patch surface. All radiative reflection and longwave emission is assumed perfectly diffuse, which enables radiative exchanges to be tracked with the use of view (or shape) factors. A ray tracing function determines whether patches are visible to each other. View factors for those patch pairs visible to one another are then calculated with the exact plane parallel analytical equations [20,46] combined with view factor algebra [53]. Downwelling longwave radiation from the sky is based on Browns sky model [3] as implemented in the ASHRAE Toolkit [33], which is a function of air and dew point temperatures, cloud cover and cloud height. A minimum of two reflections is performed, and reflections continue thereafter

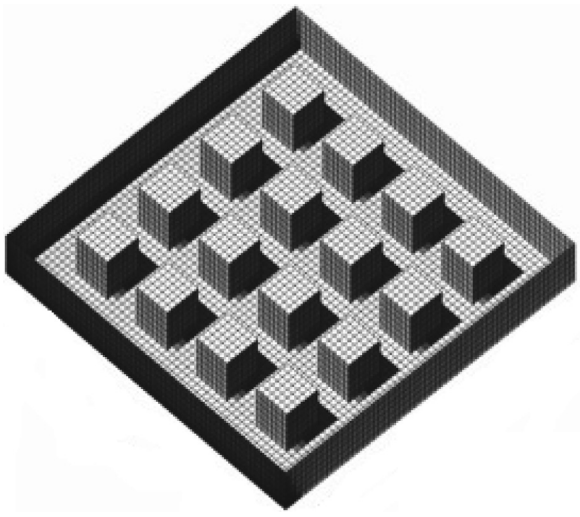

Fig. A.14. An example of the TUF-IOBES simulation domain [23,55] demonstrating the solar radiation flux at 1000 local time.

until the changes in both sub-domain averaged shortwave albedo and longwave reflectivity between reflections are less than a user-defined threshold. The transient heat conduction is solved based on the z-transform method utilizing conduction transfer functions [55], and for ground conduction, the diffusion equation by [19] is solved to obtain a sinusoidal temperature boundary condition at the surface with a constant temperature boundary condition at soil depth. The surface convective heat fluxes are simulated based on the temperature differences between surfaces and canopy air, multiplied by a convective heat transfer coefficient based on an empirical model known as the DOE-2 method. Further information on the model, including fenestration model and forcing data can be found in [55] and [23].

Krayenhoff and Voogt [23] describe a detailed validation of the radiation submodel as well as the full model test against measurements at the Vancouver Light Industrial (LI) site [27]. Additionally, the International Urban Energy Balance Model Comparison project [17] evaluated the performance of the TUF-3D model in predicting the energy balance components. With suitable input parameters, it provided reasonable agreement with measurements, comparable to a range of other commonly-used energy balance models. Lastly, in [55], the transient heat conduction simulation in TUF-IOBES is validated against an analytical solutions, while yearly and daily cooling and heating load simulations are validated against other whole building energy simulators.

References

[1] H. Akbari, H.D. Matthews, Global cooling updates: reflective roofs and pavements, Energy and Buildings 55 (2012) 2–6.
[2] U. Berardi, A. GhaffarianHoseini, A. GhaffarianHoseini, State-of-the-art analysis of the environmental benefits of green roofs, Applied Energy 115 (2014) 411–428.
[3] D.F. Brown, An improved methodology for characterizing atmospheric boundary layer turbulence and dispersion (1997).
[4] B. Bueno, L. Norford, J. Hidalgo, G. Pigeon, The urban weather generator, Journal of Building Performance Simulation 6 (4) (2013) 269–281.
[5] B. Bueno, M. Roth, L. Norford, R. Li, Computationally efficient prediction of canopy level urban air temperature at the neighbourhood scale, Urban Climate 9 (2014) 35–53.
[6] Building and Construction Authority, Singapore, Code on envelope thermal performance for buildings, 2008, (https://www.bca.gov.sg/performancebased/others/retv.pdf/).
[7] Building and Construction Authority, Singapore, BCA green mark for new non-residential buildings, 2015.
[8] B. Castellani, E. Morini, E. Anderini, M. Filipponi, F. Rossi, Development and characterization of retro-reflective colored tiles for advanced building skins, Energy and Buildings 154 (2017) 513–522.
[9] W.T. Chow, M. Roth, Temporal dynamics of the urban heat island of Singapore, International Journal of Climatology 26 (15) (2006) 2243–2260.
[10] K. Chua, S. Chou, Energy performance of residential buildings in Singapore, Energy 35 (2) (2010a) 667–678.
[11] K. Chua, S. Chou, An ETTV-based approach to improving the energy performance of commercial buildings, Energy and Buildings 42 (4) (2010b) 491–499.
[12] J. Damon, L'urbanisation mondiale en perspective positive, Études 414 (6) (2011) 739–749.
[13] C. Duarte, P. Raftery, S. Schiavon, SinBerBEST technology energy assessment report, Building Efficiency and Sustainability in the Tropics (2016).
[14] Energy Information Administration United States, 2003 commercial buildings energy consumption survey (CBECS), 2003.
[15] E. Erell, T. Williamson, Simulating air temperature in an urban street canyon in all weather conditions using measured data at a reference meteorological station, International Journal of Climatology 26 (12) (2006) 1671–1694.
[16] C. Georgakis, S. Zoras, M. Santamouris, Studying the effect of "cool" coatings in street urban canyons and its potential as a heat island mitigation technique, Sustainable Cities and Society 13 (2014) 20–31.
[17] C. Grimmond, M. Blackett, M. Best, J.-J. Baik, S. Belcher, J. Beringer, S. Bohnenstengel, I. Calmet, F. Chen, A. Coutts, et al., Initial results from phase 2 of the international urban energy balance model comparison, International Journal of Climatology 31 (2) (2011) 244–272.
[18] S. Grimmond, Urbanization and global environmental change: local effects of urban warming, Geographical Journal 173 (1) (2007) 83–88, doi:10.1111/j.1475-4959.2007.232_3.x.
[19] D. Hillel, Soil temperature and heat flow, Fundamentals of soil physics, Chapt 12 (1982) 287–317.
[20] H.C. Hottel, A.F. Sarofim, Radiative transfer, McGraw-Hill, 1967.
[21] International Business Publications, USA, Transportation policy and regulations handbook, strategic information and regulations, 2013.
[22] D.P. Johnson, J.S. Wilson, The socio-spatial dynamics of extreme urban heat events: The case of heat-related deaths in Philadelphia, Applied Geography 29 (3) (2009) 419–434.
[23] E.S. Krayenhoff, J.A. Voogt, A microscale three-dimensional urban energy balance model for studying surface temperatures, Boundary-Layer Meteorology 123 (3) (2007) 433–461.
[24] X.-X. Li, L.K. Norford, Evaluation of cool roof and vegetations in mitigating urban heat island in a tropical city, Singapore, Urban Climate 16 (2016) 59–74.
[25] Y. Liu, R. Stouffs, A. Tablada, N.H. Wong, J. Zhang, Development of micro-scale weather data on building energy consumption in Singapore, in: 4th International Conference on Countermeasures to Urban Heat Island, 2016.
[26] M. Martin, N.H. Wong, D.J.C. Hii, M. Ignatius, Comparison between simplified and detailed energyplus models coupled with an urban canopy model, Energy and Buildings (2017).
[27] V. Masson, C.S.B. Grimmond, T.R. Oke, Evaluation of the town energy balance (TEB) scheme with direct measurements from dry districts in two cities, Journal of applied meteorology 41 (10) (2002) 1011–1026.
[28] X. Meng, T. Luo, Z. Wang, W. Zhang, B. Yan, J. Ouyang, E. Long, Effect of retro-reflective materials on building indoor temperature conditions and heat flow analysis for walls, Energy and Buildings 127 (2016) 488–498.
[29] National Environmental Agency, Singapore, Household energy consumption study, 2012, (http://www.e2singapore.gov.sg/Households/Saving_Energy_At_Home/Household_Studies.aspx/).
[30] A. Niachou, K. Papakonstantinou, M. Santamouris, A. Tsangrassoulis, G. Mihalakakou, Analysis of the green roof thermal properties and investigation of its energy performance, Energy and buildings 33 (7) (2001) 719–729.
[31] J. Nichol, Visualisation of urban surface temperatures derived from satellite images, International Journal of Remote Sensing 19 (9) (1998) 1639–1649.
[32] F. Olivieri, C. Di Perna, M. D'Orazio, L. Olivieri, J. Neila, Experimental measurements and numerical model for the summer performance assessment of extensive green roofs in a Mediterranean coastal climate, Energy and Buildings 63 (2013) 1–14.
[33] C. Pedersen, R. Liesen, R. Strand, D. Fisher, L. Dong, P. Ellis, A toolkit for building load calculations; exterior heat balance (CD-ROM), American Society of Heating, Refrigerating and Air Conditioning Engineers (ASHRAE), Building Systems Laboratory (2001).
[34] Y. Qin, A review on the development of cool pavements to mitigate urban heat island effect, Renewable and Sustainable Energy Reviews 52 (2015a) 445–459.
[35] Y. Qin, Urban canyon albedo and its implication on the use of reflective cool pavements, Energy and Buildings 96 (2015b) 86–94.
[36] F. Rossi, B. Castellani, A. Presciutti, E. Morini, M. Filipponi, A. Nicolini, M. Santamouris, Retroreflective façades for urban heat island mitigation: Experimental investigation and energy evaluations, Applied Energy 145 (2015) 8–20.
[37] M. Roth, C. Jansson, E. Velasco, Multi-year energy balance and carbon dioxide fluxes over a residential neighbourhood in a tropical city, International Journal of Climatology (2016).
[38] Y.-H. Ryu, J.-J. Baik, Quantitative analysis of factors contributing to urban heat island intensity, Journal of Applied Meteorology and Climatology 51 (5) (2012) 842–854.
[39] D.J. Sailor, T.B. Elley, M. Gibson, Exploring the building energy impacts of green roof design decisions–a modeling study of buildings in four distinct climates, Journal of Building Physics 35 (4) (2012) 372–391.
[40] F. Salamanca, M. Georgescu, A. Mahalov, M. Moustaoui, A. Martilli, Citywide impacts of cool roof and rooftop solar photovoltaic deployment on near-surface air temperature and cooling energy demand, Boundary-Layer Meteorology 161 (1) (2016) 203–221.
[41] M. Santamouris, Heat island research in Europe: the state of the art, Advances in building energy research 1 (1) (2007) 123–150.
[42] M. Santamouris, Using cool pavements as a mitigation strategy to fight urban heat island–a review of the actual developments, Renewable and Sustainable Energy Reviews 26 (2013) 224–240.
[43] M. Santamouris, Cooling the cities–a review of reflective and green roof mitigation technologies to fight heat island and improve comfort in urban environments, Solar Energy 103 (2014) 682–703.
[44] M. Santamouris, Regulating the damaged thermostat of the cities–status, impacts and mitigation challenges, Energy and Buildings 91 (2015) 43–56.
[45] M. Santamouris, A. Synnefa, T. Karlessi, Using advanced cool materials in the urban built environment to mitigate heat islands and improve thermal comfort conditions, Solar Energy 85 (12) (2011) 3085–3102.
[46] R. Siegel, J. Howell, Thermal radiation heat transfer, 1, CRC press, 2001.
[47] I.D. Stewart, T.R. Oke, Local climate zones for urban temperature studies, Bulletin of the American Meteorological Society 93 (12) (2012) 1879–1900.
[48] A. Synnefa, M. Santamouris, H. Akbari, Estimating the effect of using cool coatings on energy loads and thermal comfort in residential buildings in various climatic conditions, Energy and Buildings 39 (11) (2007) 1167–1174.
[49] H. Taha, H. Akbari, A. Rosenfeld, J. Huang, Residential cooling loads and the urban heat island–the effects of albedo, Building and environment 23 (4) (1988) 271–283.
[50] D. Wang, A. Ukil, U. Manandhar, Building HVAC load profiling using energyplus, in: 7th IEEE Innovative Smart Grid Technologies Conf., ISGT, 2015.

[51] Windows and Daylighting Group, Lawrence Berkeley Laboratory, Window 7.4, 2013, (https://windows.lbl.gov/software/window/).
[52] N.H. Wong, Y.P. Tan, L.F. Loh, Historical analysis of long-term climatic data to study urban heat island in Singapore, Architectural Science Review 48 (1) (2005) 25–40.
[53] L. Wu, Urban4: An urban canopy layer surface energy balance climate model (1995).
[54] N. Yaghoobian, J. Kleissl, Effect of reflective pavements on building energy use, Urban Climate 2 (2012a) 25–42.
[55] N. Yaghoobian, J. Kleissl, An indoor–outdoor building energy simulator to study urban modification effects on building energy use–model description and validation, Energy and Buildings 54 (2012b) 407–417.
[56] J. Yang, Z.-H. Wang, K.E. Kaloush, Environmental impacts of reflective materials: Is high albedo a “silver bullet” for mitigating urban heat island? Renewable and Sustainable Energy Reviews 47 (2015) 830–843.
[57] N. Negin, J. Kleissl, CFD simulation of an idealized urban environment: thermal effects of geometrical characteristics and surface materials, Urban Climate, 12, 2015, pp. 141–159.